# Chemical Genetics Approach to Identify Peptide Ligands that Selectively Stimulate DAPK-1 Kinase Activity

Jennifer A. Fraser and Ted R. Hupp*

*Cancer Research UK p53 Signal Transduction Group, University of Edinburgh Cancer Research Centre, Western General Hospital, Crewe Road South, Edinburgh EH4 2XR, U.K.*

*Received August 2, 2006; Revised Manuscript Received November 15, 2006*

ABSTRACT: Dissection of signal transduction pathways has been advanced by classic genetic approaches including targeted gene deletion and siRNA-based inhibition of gene product synthesis. Chemical genetics is a biochemical approach to develop small peptide-mimetic ligands to alter, post-translationally, how an enzyme functions. DAPK-1 was used as a model enzyme to develop selective peptide ligands that modulate its specific activity. The tumor modifier p21 has the most highly conserved elements of a DAPK consensus substrate, including a basic core followed by a hydrophobic core. Therefore, the p21 protein was synthesized in overlapping fragments to acquire a panel of peptide ligands for testing in DAPK binding and phosphorylation assays. Three distinct p21 derived peptide fragments were found to bind to DAPK; however, these had no stimulatory effect on its activity toward *in vivo* substrates, p21 and MLC. The p21 peptide ligands did, however, strikingly stimulate DAPK activity toward p53, a substrate that shows conservation in the hydrophobic part of its DAPK-1 consensus site. DAPK-1 stimulatory peptides attenuate tryptic cleavage of DAPK-1, suggesting that ligand binding can alter DAPK-1 conformation and lock the enzyme onto its substrate. We, therefore, generated an artificial p53, containing arginine residues N-terminal to the phospho-acceptor site, creating a better DAPK-1 peptide consensus and demonstrated that the $K_m$ for $p53^{1-66[ET\rightarrow RR]}$ and ATP is elevated. The full-length $p53^{E17T18\rightarrow R17R18}$ also functioned as a better $Ser^{20}$ kinase substrate *in vivo*. These data suggest that DAPK-1 binding ligands can be generated to elevate its specific activity toward weak substrates and provide an approach to develop genetic assays to alter DAPK-1-specific activity *in vivo*.

Genetic approaches have been used classically to dissect signal transduction pathways using techniques including recombination-based gene deletion and siRNA vectors. However, depletion of total protein prevents analysis of subtle branched signaling that represents the multi-component function of a protein. Chemical genetics is a combined biochemical and reverse genetics approach to develop small peptide-mimetic ligands to alter how an enzyme functions (*1*). Some of the first indications that peptides could be used as genetic tools came from studies showing that the disruption of protein−protein interactions may lead to therapeutic effects. Protein targets have included RAS, Cyclins, CDKs, and MDM2 (*2*−*5*). The ability of small peptides to function reflect the growing concept that many protein−protein interactions are stabilized by small linear interaction motifs, sometimes as small as four amino acids. Peptide ligands can thus reflect a new protein−protein interface, a regulatable protein−protein interface, and/or a lead for target validation for inhibiting pathways in cells. However, peptide ligands can also be used to stimulate the function of a protein by allosteric mechanisms. The binding of peptide to the active site of p53 can induce a conformational more compatible for DNA-binding *in vitro* (*6*). Furthermore, a more recent approach has identified an allosteric stimulation of MDM2 function as an E3-Ubiquitin ligase by peptide ligands, providing evidence that chemical genetic approaches can also be used to stimulate rather than inhibit enzyme function (*7*). Whether stimulatory peptide ligands can be generated toward other enzymes such as protein kinases is possible given that growing evidence suggests that protein kinases can function in part through docking sites that allosterically activate the enzyme toward substrates (*8*).

In an effort to begin to develop novel peptide ligands that are stimulatory for enzyme function, we focused on the calcium calmodulin kinase superfamily members that are genetic activators of the p53 pathway, Chk2 and DAPK-1[1]. The mechanism of Chk2 activation of p53 is biochemically well defined, and Chk2 has already been shown to display significant dependence on a docking interaction to modify the p53 activation domain (*9*). However, the DAPK-1 mechanism of p53 activation is not defined mechanistically, nor is it known whether the core kinase domain can function through docking-dependent interactions.

DAPK-1 belongs to a novel family of ubiquitously expressed pro-apoptotic kinases that also contains DAPK-2 (also known as DRP 1), DAPK-3 (also known as ZIPK),

* Corresponding author. Tel: 44-131-777-3500. Fax: 44-131-777-3583. E-mail: Ted.Hupp@ed.ac.uk.

[1] Abbreviations: BSA, bovine serum albumin; CaM, calmodulin; CK, casein kinase; DAPK, death associated protein kinase; ELISA, enzyme linked immunosorbant assay; IVT, *in vitro* translation; $MLC_{20}$, myosin light chain; PBST, phosphate buffered saline with Tween; WT; wild type, ZIPK, zipper-interacting protein.

10.1021/bi061562j CCC: $37.00 
Published on Web 02/13/2007

and DAPK-related protein 1 and 2 (DRAK-1 and -2) (*10*). Although the DAPK family members all differ in size and structure, they share a high degree of homology in the catalytic kinase domain. This domain also shows significant identity (44%) with the kinase domains of calmodulin (CaM) regulated kinases, in particular myosin light chain kinase. DAPK members differ from other CaM-regulated kinases because of the presence of a unique stretch of 12 amino acids found within the catalytic domain, which is enriched in basic residues. This is recognized as the "finger print" of DAPK family members and shares a high degree of homology between all five kinases. The crystal structure of DAPK has been solved by mapping onto phosphorylase kinase (*11*, *12*), and an analysis of the structure indicates that the basic loop protrudes from the surface of DAPK and is positioned over the putative peptide-binding domain. It has, therefore, been suggested that the basic loop may play a role in substrate recognition or enzyme regulation; however, this has not yet been demonstrated. Analyses of co-crystalized DAPK has uncovered the potential residues involved in ATP binding and has led to the development of small molecule inhibitors of DAPK (*13*). Use of these inhibitors *in vivo* has given remarkable insights into the function of DAPK, in particular its role in the central nervous system. In the adult mouse, DAPK is expressed abundantly in the brain, particularly the hippocampus, cerebral cortex, and cerebellum. DAPK mRNA expression in these areas was found to be dramatically elevated following transient ischemeic injury (*14*, *15*). This is accompanied by an increase in the specific activity of DAPK in damaged regions (*16*), suggesting that DAPK may play a role in apoptotic cell death following traumatic injury. The importance of DAPK in neuronal cell death is highlighted by the use of neurons derived from DAPK knockout mice. In the absence of DAPK, retinal ganglion cells show enhanced ability to survive exposure to cytotoxic levels of extracellular glutamate; a model of cellular excitotoxicity (*17*), whereas apoptotic cell death following treatment with high levels of ceramide was abrogated in cultured hippocampal neurons lacking DAPK (*18*). These findings suggest DAPK becomes activated in response to several forms of neuronal injury, triggering neuronal cell death, and highlights the potential for the manipulation of DAPK activity as a therapeutic target in order to offer neuroprotection. Indeed, injection of small molecule inhibitors of DAPK such as 3-amino-6-phenylhydrazine prior to or 6 h post ischemeic injury is sufficient to protect against the loss of neuronal tissue *in vivo* (*19*).

DAPK-1 is used in this article as a model enzyme with which to develop selective peptide ligands that modulate its specific activity. Given that many enzymes exhibit multifaceted docking sites for substrate phosphorylation, we generated a library of synthetic peptide ligands derived from the DAPK substrate $p21^{WAF1/CIP}$ (p21) and tested them using DAPK binding and phosphorylation assays. Three distinct p21-derived peptide fragments were found to bind DAPK. Although these ligands were unable to stimulate DAPK specific activity toward its *in vivo* substrates, $MLC_{20}$ and p21, they were able to stimulate DAPK-1 activity toward p53, a substrate that contains a partially conserved DAPK-1 consensus site. Data are presented suggesting that the stimulatory peptide ligands of DAPK-1 alter its conformation and $K_m$ for substrates, providing evidence that DAPK-1 can be used as a model kinase for the design of ligands that can in future be used for modifying enzyme activity *in vivo*.

## EXPERIMENTAL PROCEDURES

*Peptides and Substrates.* Peptides were synthesized as N-terminal biotinylated peptides with SGSG spacers and were obtained from Mimotopes Pty., Ltd. (Clayton, Australia). Peptides were dissolved in $Me_2SO$ and stored at −20 °C. Recombinant human p21 and ZIPK were expressed in arabinose-inducible BL21 *E. coli* and purified as previously described (*21*, *22*). Rabbit muscle myosin and myosin light chain ($MLC_{20}$) were obtained from Sigma.

*Site-Directed Mutagenesis.* Amino acid mutations were introduced into wild-type $p53^{1-66}$ at $Glu^{17}$ and $Thr^{18}$ according to the QuikChange mutagenesis kit (Stratagene) using pGEX $p53^{1-66}$ and pcDNA3.1 p53 as a template and the following sets of complimentary oligonucleotides designed to introduce base changes (underlined):

p53 1−66 ET → KK FP 5′ CCTCTGAGTCAGAAAAAATTTTCAGACCTA 3′;

p53 1−66 ET → KK RP 5′ GATGTCTGAAAATTTTTTCTGACTCAGAGG 3′;

p53 1−66 ET → RR FP 5′ CCTCTGAGTCAGCGAAGATTTTCAGACCTA 3′;

p53 1−66 ET → RR RP 5′ TAGGTCTGAAAATCTTCGCTGACTCAGAGG 3′.

The presence of mutations was verified by sequencing.

*Expression and Purification of Recombinant Mutant $p53^{1-66}$ from Bacteria.* GEX $p53^{1-66}$ wild type, KK, and RR ($p53^{1-66[ET\rightarrow KK]}$ or $p53^{1-66[ET\rightarrow RR]}$) were used to transform BL21 AI *E. coli*. Large-scale cultures containing ampicillin (100 μg/mL) were grown with shaking at 37 °C to an $OD_{600}$ of 0.5. Recombinant protein expression was induced by the addition of arabinose to a final concentration of 0.2%, and cultures were grown for a further 3 h at 30 °C. Cells were harvested by centrifugation at 3000 rpm, and cell pellets were resuspended in 25 mM Hepes at pH 7.5, 10% sucrose, 300 mM NaCl, 5 mM dithiothreitol, 5 mM benzamidine and protease inhibitors cocktail (Roche). Lysozyme was added to a final concentration of 1 mM, and the lysates were mixed by rotation for 20 min at 4 °C. The lysates were further subjected to freeze−thaw in liquid nitrogen and sonication before they were clarified by centrifugation at 13 000 rpm at 4 °C. Recombinant GST-tagged proteins were purified from clarified lysates using glutathione sepharose according to the manufacturer's instructions (Amersham Pharmacia). Purified protein concentrations were determined by Bradford (*20*) or BCA assay (Novagen).

*Insect Cell Expression of the DAPK Core.* pDEST 20 DAPK core (residues 1−278) was transformed into DH10BAC *E.coli* according to the manufacturer's instructions. Sf9 cells were grown in Sf900-II medium containing glutamine (Invitrogen) in spinner flasks at 26 °C. Recombinant bacmid DNA was isolated and used to transfect Sf9 insect cells. DAPK core was expressed by infecting Sf9 cells with viral stock, and 72 h post infection, cell pellets were collected by centrifugation. Cell pellets were resuspended in 25 mM Hepes at pH 7.5, 400 mM KCl, 1 mM DTT, 1 mM benzamidine, and 1% NP-40 containing 1 mM Na pyruvate, 10 mM glycerol phosphate, 0.25 mM NaF, and protease inhibitors (Roche) and incubated on ice for 30 min. Lysates

were further subjected to freeze−thaw in liquid nitrogen and sonication before they were clarified by cold centrifugation at 13 000 rpm. Recombinant GST-tagged DAPK was purified from clarified insect cell lysates using glutathione sepharose according to the manufacturer's instructions (Amersham Biosciences)

*Kinase Assays in Vitro.* Purified recombinant enzyme (∼200 ng) was incubated with substrate (150 ng of p21, $p53^{1-66}$, and $MLC_{20}$ or 1 $\mu$g of whole myosin unless otherwise stated) and 1 $\mu$g of peptides (∼50 $\mu$M final concentration), where indicated, in reaction buffer (50 mM Hepes at pH 7.5, 10 mM $MgCl_2$, 1 mM dithiothreitol, and 0.8 mM EDTA) containing 0.1 mM $\beta$-glycerol phosphate in a final volume of 9 $\mu$L. The reactions were initiated by the addition of 1 $\mu$L of ATP (1:50 dilution of [$\gamma^{32}$P] ATP (3000 Ci/mmol) in 2 mM ATP) and incubated at 30 °C for 30 min. The reactions were terminated by the addition of the Laemmli sample buffer and resolved by SDS−PAGE. Gels were dried, and [$\gamma^{32}$P]ATP incorporation into reaction products was visualized by autoradiography. Dried gels were also exposed to a storage phosphor screen (Amersham) overnight, and [$\gamma^{32}$P]ATP incorporation was quantified via a phosphorimager (Storm 840, Amersham Biosciences). The actual counts of [$\gamma^{32}$P]ATP incorporated into the reaction products was determined from a [$\gamma^{32}$P]ATP standard curve. The concentrations of wild-type and KK mutant $p53^{1-66}$ [$p53^{1-66[ET\rightarrow KK]}$] ranging from 0.018 to 2.48 $\mu$M or 0.08 to 10.33 $\mu$M for RR mutant $p53^{1-66}$ [$p53^{1-66[ET\rightarrow RR]}$] were used to determine the $K_m$ and $V_{max}$ values. The $K_m$ and $V_{max}$ values for ATP in the presence of the $p53^{1-66}$ wild type were determined from kinase reactions containing concentrations of ATP ranging from 0.02 to 200 $\mu$M and saturating concentrations of $p53^{1-66}$ wild type (0.6 $\mu$M). Because of the high $K_m$ value obtained for $p53^{1-66}$ RR [$p53^{1-66[ET\rightarrow RR]}$], a concentration from the linear range was chosen (2.4 $\mu$M) to determine the $K_m$ and $V_{max}$ values for ATP in its presence. For the purpose of determining the kinetic parameters of ATP, serial dilutions of the stock [$\gamma^{32}$P]ATP mix were generated and used to initiate kinase reactions as above. Michaelis−Menten parameters were fitted via the Hanes plot using hyperbolic regression analysis software (Hyper, version 1.1s, J. Easterby, University of Liverpool). and kinetic constants were calculated as the mean ± the standard deviation. In the absence of the radiolabel, reactions were initiated with cold ATP to a final concentration of 0.2 mM. The reaction products were resolved and transferred to nitrocellulose, and phosphorylation of p21 was detected via Western blotting using αp21-phospho-$Thr^{145}$ IgG or αp21-phospho-$Ser^{146}$ IgG at a 1:1000 dilution, as previously described (*21*).

*Enzyme-Linked Immunosorbent Assay.* For the GST capture of p21 peptides via GST-tagged recombinant protein, microtiter plates were coated in GST IgG (Sigma, 1:250 dilution in 3% BSA in PBS containing 0.1% Tween 20 (PBST)) overnight at 4 °C. After washing with PBST, the wells were incubated with 200 nM recombinant GST DAPK or ZIPK in a final volume of 50 $\mu$L of 3% BSA PBST for 1 h at room temperature. The wells were blocked with 3% BSA/PBST for 1 h and incubated with 100 ng (final concentration of 50 $\mu$M) of p21 peptide in 3% BSA/PBST. After an hour at room temperature, the wells were washed and incubated with anti streptavidin IgG HRP conjugate (Sigma) diluted 1:1000 in 3% BSA/PBST for a further hour. After extensive washing with PBST, bound IgG was detected using ECL solution and analyzed using an Ascent Fluouroskan plate reader (Labsystems) at 450 nm. For the streptavidin capture of biotinylated p21 20-mer peptides, microtiter plates were coated with 0.1 $\mu$g of streptavidin in water overnight at 37 °C. After washing with PBST, the wells were incubated for 1 h with 100 ng of peptide diluted in 3% BSA/PBST. The wells were washed with PBST and blocked with 3% BSA/PBST. Plates were then coated with 200 nM recombinant GST-tagged DAPK or ZIPK in a final volume of 50 $\mu$L of 3% BSA PBST for 1 h at room temperature. The wells were incubated with anti-GST IgG (Sigma) diluted 1:1000 in 3% BSA/PBST for an hour followed by HRP-conjugated rabbit anti-mouse IgG (Dako) diluted 1:1000 in 3% BSA/PBST for a further hour. The wells were washed extensively in between incubations, and bound IgG was detected using ECL as above.

*Transcription and Translation of DAPK and ZIPK in Vitro.* DAPK and ZIPK were translated *in vitro* using the TnT T7-coupled reticulocyte lysate system (Promega). Coupled transcription/translation was carried out at 30 °C for 90 min according to the manufacturer's protocol, using 1 $\mu$g of pDEST 14 and pDEST 15 constructs containing either ZIPK or DAPK (full-length and core domain) as DNA templates in a reaction mixture of 50 $\mu$L. The translated products were radio-labeled with Redivue L-[$^{35}$S]methionine (Amersham) and analyzed by SDS−PAGE and autoradiography.

*Partial Tryptic Digestion of in vitro Translated Products.* A 100 ng/$\mu$L stock solution of trypsin (Roche) was prepared in 10 mM HCl. The translated protein (1 $\mu$L of the TnT T7 reaction mix) or purified $p53^{1-66}$ (300 ng) was incubated with 10 or 1 ng/$\mu$L trypsin in reaction buffer (50 mM Hepes at pH 7.5, 10 mM $MgCl_2$, 1 mM dithiothreitol (DTT), and 0.8 mM EDTA) in the presence or absence of 1 $\mu$g (50 $\mu$M) of p21 peptide for 30 min on ice. The reactions were stopped by the addition of the Laemmli sample buffer and resolved by SDS−PAGE, and tryptic fragments were analyzed by autoradiography. In the case of $p53^{1-66}$, the tryptic fragments were resolved using 15% SDS−PAGE and detected by silver staining.

*Cell Culture, Transfection, Lysis, and Analysis.* H1299 cells were cultured in RPMI 1640 medium (Invitrogen) supplemented with 5% foetal bovine serum at 37 °C with 5% $CO_2$. Cells were seeded 24 h prior to transfection at a density of $1 \times 10^5$ cell/mL in 6-well dishes and transfected with the indicated concentration of pcDNA 3.1 or pcDNA 3.1 p53 WT, or p53 RR mutant using lipofectamine 2000 (Invitrogen). Cells were harvested 24 h after transfection by scraping into phosphate buffered saline, and cells were collected by low-speed centrifugation at 4 °C. Cell pellets were lysed with 3 volumes of urea lysis buffer (6 M urea, 20 mM Hepes at pH 8.0, 25 mM NaCl, 100 mM DTT, and 0.5% Triton X) for 30 min on ice and clarified by cold centrifugation at 13 000 rpm in a bench top centrifuge. The protein concentration of the lysates was determined by Bradford analysis, and samples were prepared using the Laemmli sample buffer to a final concentration of 1 mg/mL. Lysates were resolved using 12% SDS−PAGE and transferred onto nitrocellulose membranes as previously described (*21*). Total p53 protein levels were detected by Western blotting using D0-12 at 1:1000 dilution in 5% nonfat

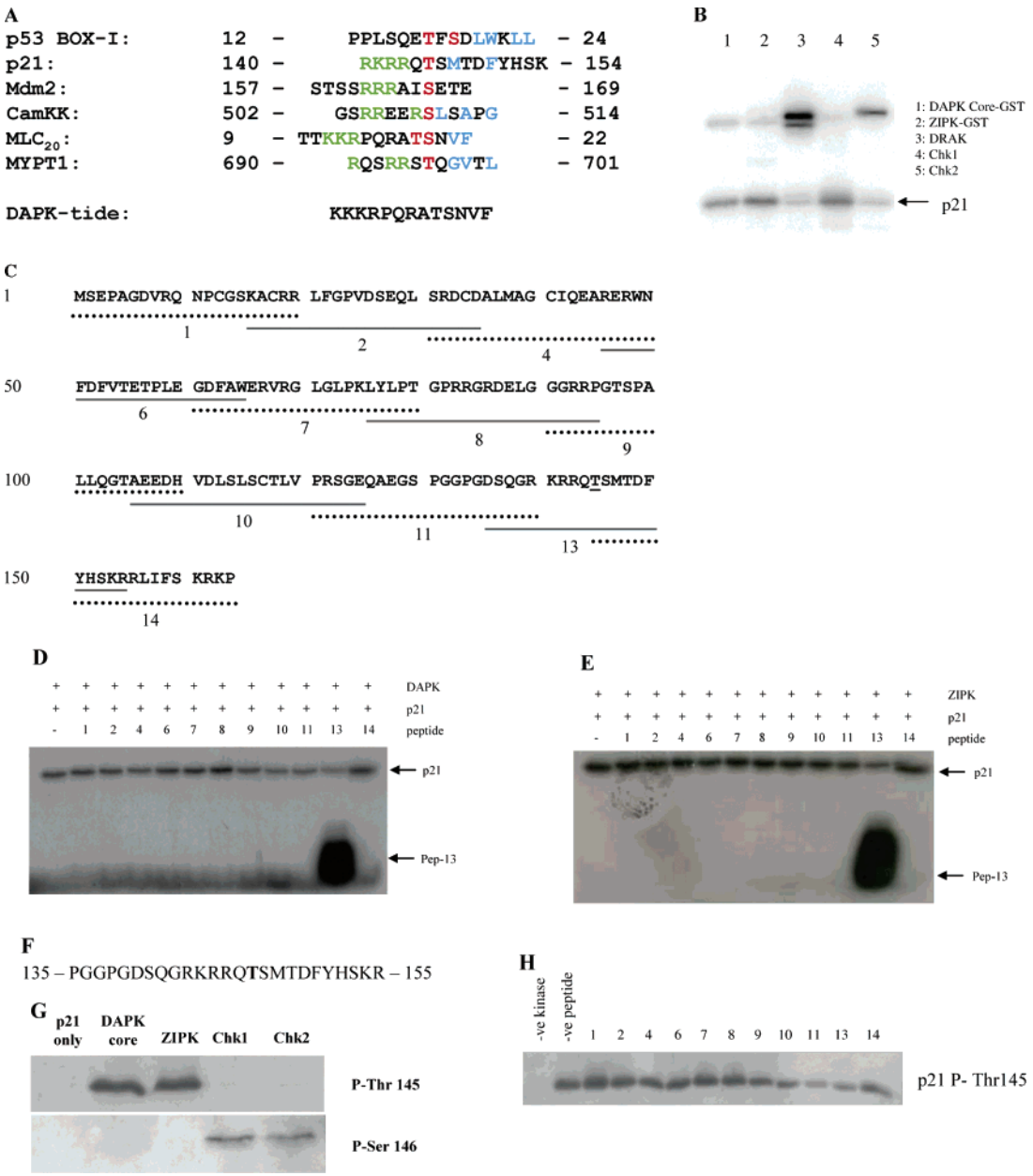


FIGURE 1: DAPK core is highly active toward p21$^{WAF1}$ *in vitro*. (A) Comparison of the homology of peptide consensus sequences for known and potential DAPK substrates. The sequences in red signify the phospho-acceptor sites, the basic residues are in green, and the hydrophobic residues are in blue. (B) Comparison of DAPK core, ZIPK, DRAK, Chk1, Chk2, and AMPK activity toward p21. Kinase reactions containing [$\gamma^{32}$P]ATP and 150 ng of p21 were assembled in the presence of the indicated kinases and incubated for 30 min at 30 °C. The reaction products were resolved by SDS−PAGE, and [$\gamma^{32}$P]ATP incorporation was visualized by autoradiography. (C) Positioning of the biotinylated p21 20-mer peptides on full-length p21. (D and E) p21 20-mer peptide 13 is phosphorylated by purified DAPK core (D) and ZIPK (E). Kinase reactions containing [$\gamma^{32}$P]ATP and 150 ng of p21 were assembled with 1 $\mu$g of the indicated p21 20-mer peptides (final peptide concentration ~50 $\mu$M) and incubated for 30 min at 30 °C. The reaction products were resolved by 15% SDS−PAGE, and [$\gamma^{32}$P]ATP incorporation was visualized by autoradiography. (F) Amino acid sequence of p21 peptide 13. The Thr$^{145}$ phospho-acceptor site is highlighted in bold. (G) Western blot analyses of p21 phosphorylation by various kinases. Kinase reactions were assembled as in (A) with cold ATP and incubated for 30 min at 30 °C. The reaction products were resolved and transferred to nitrocellulose. Phosphorylation was detected using αp21-phospho-Thr$^{145}$ IgG or αp21-phospho-Ser$^{146}$ IgG. (H) p21 peptides compete with DAPK for the phosphorylation of full-length p21 at Thr$^{145}$. The reactions containing DAPK, full-length p21, and the indicated p21 peptides were assembled as in (G) and analyzed for the presence of Thr$^{145}$ phosphorylation by Western blotting.

milk, and p53 phosphorylation at Ser$^{20}$ was detected using αp53-Pser$^{20}$ IgG (Santa Cruz) at 1:1000 dilution in 3% BSA.

## RESULTS

Studies have shown that DAPK/ZIPK has a preference for basic residues such as arginine and lysine upstream of the serine/threonine phosphorylation site (*11*) (Figure 1). Downstream of the phospho-acceptor site, substrates targeted by DAPK members appear to be rich in hydrophobic residues, such as leucine, valine, and phenylalanine (*22*). These data suggest that DAPK has a large contact site with substrates.

A comparison of peptide consensus sites for several known DAPK family substrates (Figure 1A) to open reading frames in the human genome indicates that the cell cycle inhibitor, p21, has the highest conservation of these basic and

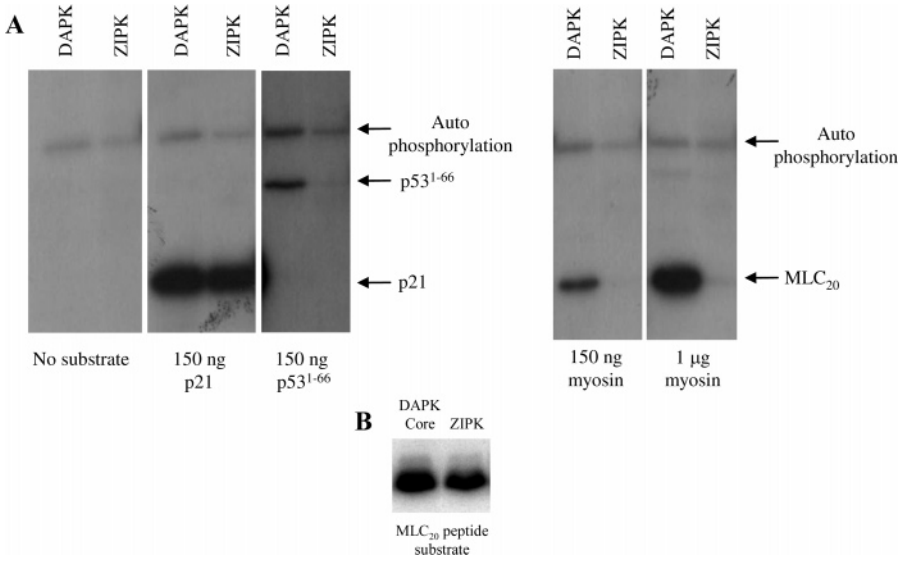


FIGURE 2: DAPK core and ZIPK are weakly active toward p53$^{1-66}$. (A) Comparison of DAPK core and ZIPK utilization of p21, p53$^{1-66}$, and myosin. Kinase reactions containing [$\gamma^{32}$P]ATP, DAPK core, or ZIPK and the indicated concentration of substrate were assembled and incubated for 30 min at 30 °C. The reaction products were resolved by 12% SDS−PAGE, and [$\gamma^{32}$P] ATP incorporation was visualized by autoradiography. (B) Comparison of DAPK core and ZIPK activity toward MLC$_{20}$ peptide substrate. The reactions containing 1 $\mu$g of MLC$_{20}$ peptide substrate (9-TKKPRQRATSSNVFAM-24) DAPK core or ZIPK were assembled as in (A). The reaction products were resolved by 18% SDS−PAGE and analyzed by autoradiography.

hydrophobic elements, suggesting that p21 would be an excellent substrate for DAPK-1. Indeed ZIPK has been shown to phosphorylate p21 *in vitro* and *in vivo* (*22*). Because the kinase domain of DAPK-1 shares 83% identity with ZIPK, it is possible that they share commonalities in substrate utilization and that DAPK-1 may be an effective kinase toward p21 as well. DAPK-1 is a complex multidomain protein, which, in addition to the kinase domain, contains a calmodulin binding motif that regulates enzyme activity, protein−protein interaction motifs, such as death domain and ankyrin repeats, as well as cytoskeletal binding domains. DAPK core was used rather than full length DAPK-1 in this study because this construct contains only the kinase domain (residues 1−277) and permits analyses of the basic requirements for DAPK catalysis and regulation without the higher levels of complexity and regulation afforded by the extra catalytic domains.

A comparison of DAPK core activity toward p21 with that of ZIPK, DRAK, Chk1, and Chk2 shows that DAPK core is an effective kinase toward p21, and the level of [$\gamma^{32}$P]-ATP phosphate incorporation into p21 by DAPK core is comparable to that of ZIPK and Chk1 (Figure 1B, compare lane 1 with lanes 2 and 4). In contrast, the more distantly related DAPK family member DRAK, which shares only 50% identity at the kinase domain, and Chk2 were much poorer kinases toward p21 (Figure 1B, lanes 3 and 5, respectively). Chk2 has been shown to phosphorylate p21 at Ser$^{146}$ (*9*); however, Chk2 activity toward p21 is weak and requires allosteric activation to enhance its activity (see below). In order to further study DAPK core activity toward p21, we synthesized p21 as peptide-overlapping fragments (Figure 1C). We found that only one of the synthetic p21 peptides, peptide 13, was effectively phosphorylated by DAPK core *in vitro* (Figure 1D). Peptide 13 contains both the Thr$^{145}$ and Ser$^{146}$ phospho-acceptor sites (Figure 1F) known to be targeted by other kinases, including ZIPK ((*22*) and Figure 1E), Chk2, PKC, and PKA (*9*, *21*). To establish which of these sites DAPK core targets on full-length p21, we used phospho-specific antiserum toward Thr$^{145}$ and Ser$^{146}$. Western blot analyses clearly show that DAPK core, like ZIPK, specifically targets the Thr$^{145}$ site in full-length p21 (Figure 1G), whereas the stress kinases, Chk1 and Chk2, target Ser$^{146}$. In the presence of peptide 13, [$\gamma^{32}$P]ATP incorporation into full-length p21 by both DAPK core and ZIPK is reduced (Figure 1D and E). More specifically, phosphorylation at Thr$^{145}$ was also reduced (Figure 1H). This is probably a result of competition between full-length and peptide substrate binding toward the enzyme. Notably, none of the p21 peptides used in this study enhanced DAPK core or ZIPK activity toward full-length p21. This is possibly because the region surrounding the Thr$^{145}$ phospho-acceptor site on p21 contains the correct elements required for efficient substrate binding and utilization by DAPK and ZIPK, and therefore, activity is maximal.

A comparison of DAPK core and ZIPK activity toward p21 and the Box I domain of p53 (p53$^{1-66}$) shows that DAPK core is not as active toward p53$^{1-66}$ as it is to p21 (Figure 2), and the extent of [$\gamma^{32}$P]ATP incorporation into p53$^{1-66}$ by DAPK core is approximately ~3-fold lower than that of p21. In contrast, p53$^{1-66}$ is very weakly phosphorylated by ZIPK, and [$\gamma^{32}$P]ATP incorporation into p53$^{1-66}$ is barely detectable compared to that of DAPK core. An analysis of the consensus sequence of p53 indicates that the conservation of the important regions surrounding the phospho-acceptor site Ser$^{20}$ is not as good for p53 as it is for p21 (Figure 1A). Although p53 contains hydrophobic residues downstream of Ser$^{20}$, the upstream region appears to lack the basic lysine and arginine residues required for efficient substrate binding. Because these residues are thought to be important for binding to the substrate binding site, their absence may account for the lower level of phosphorylation of p53$^{1-66}$ by DAPK core and ZIPK compared to that of p21 (see below, Figure 8).

DAPK core and ZIPK activity was also tested toward their classical substrate, myosin light chain, MLC$_{20}$, using whole myosin from rabbit muscle; a 480 kDa complex consisting

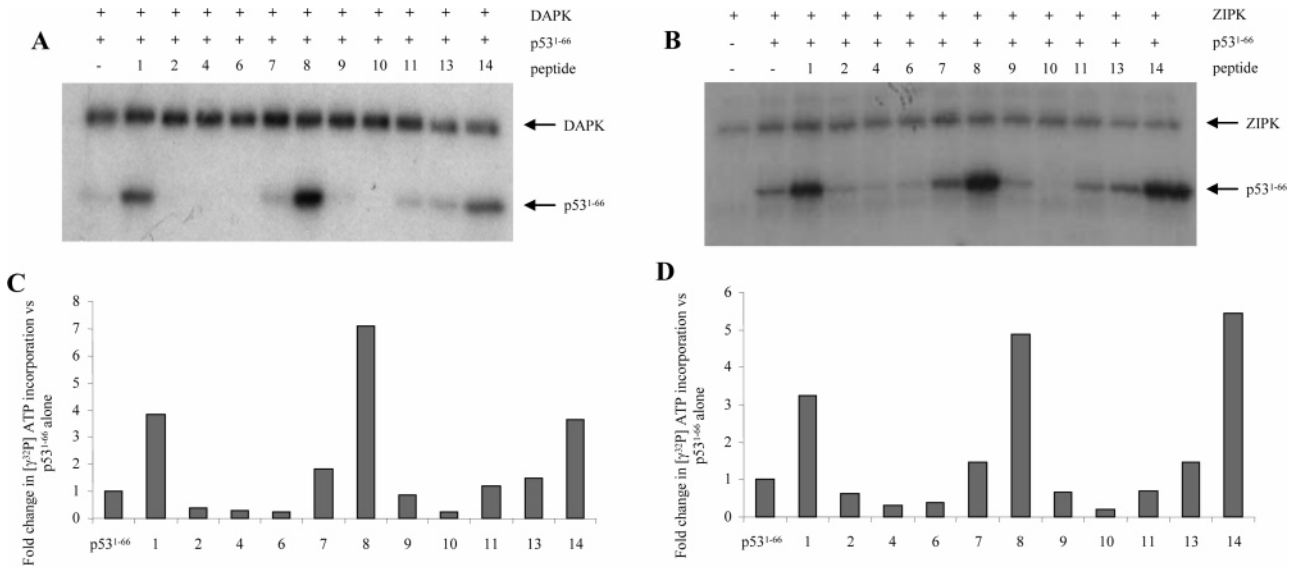


FIGURE 3: DAPK core and ZIPK activity toward $p53^{1-66}$ is stimulated by p21 peptides. Kinase reactions containing [$\gamma^{32}$P] ATP, 150 ng of $p53^{1-66}$, DAPK (A), or ZIPK (B) were assembled in the presence of the indicated p21 20-mer peptides (final peptide concentration ~50 $\mu$M). The samples were resolved by 12% SDS−PAGE, and reaction products were analyzed by autoradiography. (C and D) The intensity of [$\gamma^{32}$P]ATP incorporation into $p53^{1-66}$ was quantified by phosphorimager (STORM 840, Amersham) and normalized to $p53^{1-66}$ phosphorylation in the absence of the peptide.

of two heavy chains (200 kDa) and four light chains (17−20 kDa) and two essential and two regulatory light chains. When myosin is resolved by SDS−PAGE, the light chains resolve as a single band with an approximate molecular weight of ~20. In the presence of DAPK core or ZIPK only the ~20 kDa band is labeled with [$\gamma^{32}$P]ATP (Figure 2A), and phosphorylation of the heavy chains is not observed. The level of $MLC_{20}$ phosphorylation in the presence of DAPK core is comparable to that obtained using $p53^{1-66}$ yet still approximately ~1/3 of the signal observed in the presence of an equivalent concentration of p21 (Figure 2). Similar to that of $p53^{1-66}$, ZIPK activity toward $MLC_{20}$ was very weak, and the phosphorylated $MLC_{20}$ band was barely detectable (Figure 2A). Indeed, phosphorylation of $MLC_{20}$ by ZIPK was only observed when ZIPK was incubated with 1 $\mu$g of myosin. These findings suggest that the ZIPK used in this study is weakly active toward $MLC_{20}$ compared to DAPK core. However, in the presence of an $MLC_{20}$ peptide substrate containing the $Thr^{18}$ and $Ser^{19}$ phosphorylation sites (9-TKKPRQRA**TS**SNVFAM-24), comparable levels of ZIPK and DAPK core activity were observed (Figure 2B). This suggests factors such as $MLC_{20}$ secondary structure may be responsible for the low levels of ZIPK activity toward $MLC_{20}$ observed here.

Several studies with kinases such as MAPK have discovered that in addition to the primary phosphorylation site(s) on a substrate, there is a secondary site or region that determines enzyme activity or specificity via binding or docking to the enzyme (*8*). Indeed, allosteric activation of the enzyme toward weak substrates has been observed for several kinases, including Chk2 (*9*). We, therefore, wanted to assess whether it is possible to allosterically enhance DAPK core and ZIPK activity toward weaker substrates such as $p53^{1-66}$ and $MLC_{20}$ in a docking-dependent manner, using potential docking regions from other high-affinity substrates such as p21.

To test this, we took the overlapping p21 synthetic peptides and analyzed them for their potential to enhance DAPK core and ZIPK activity toward $p53^{1-66}$. Surprisingly, three distinct regions of p21 were capable of enhancing $p53^{1-66}$ phosphorylation by both DAPK and ZIPK (Figure 3A and B): the N-terminal 20 amino acids (peptide 1), the central region (peptides 7 and 8; residues 60−95), and the carboxyl terminal region (peptides 11, 13, and 14; residues 120−164). Activity in the presence of these peptides was dramatically greater than that of DAPK or ZIPK alone with [$\gamma^{32}$P]ATP incorporation increased by as much as 8-fold (Figure 3C and D).

To establish whether p21 peptides stimulation of activity was specific for $p53^{1-66}$, we analyzed the ability of the peptides to activate DAPK core and ZIPK activity toward $MLC_{20}$. Surprisingly, p21 peptides had little stimulatory effect on $MLC_{20}$ phosphorylation by either DAPK core or ZIPK, and in contrast to $p53^{1-66}$, p21 peptides appeared to inhibit DAPK core and ZIPK activity toward $MLC_{20}$. This was particularly apparent in the presence of peptides 1, 8, and 14 (Figure 4A and B). Peptide 13 also reduced $MLC_{20}$ labeling with [$\gamma^{32}$P]ATP; however, because DAPK core and ZIPK use peptide 13 as a substrate, the observed reduction in $MLC_{20}$ phosphorylation is probably due to competition for binding at the active site. The inhibitory effects of the p21 peptides toward DAPK core and ZIPK were more apparent when isolated $MLC_{20}$ was used as a substrate. When isolated rabbit muscle $MLC_{20}$ is resolved by 15% SDS−PAGE, three bands are clearly visible (Figure 4C) with apparent molecular weights of 23, 20, and 17. These correspond to the regulatory light chains 23 and 20 kDa and the essential light chains 17 kDa. In the presence of DAPK core or ZIPK only the 23 and 20 kDa regulatory $MLC_{20}$ bands are phosphorylated (Figure 4D and E). This is in keeping with the observation that DAPK and ZIPK phosphorylate $MLC_{20}$ regulatory chains at $Ser^{19}$ (and $Thr^{18}$ for ZIPK, (*23*, *24*)) and that the essential light chains do not undergo post-translational modification. [$\gamma^{32}$P]ATP incorporation into both regulatory 23 and 20 kDa bands was reduced in the presence of peptides 1, 8, 13, and 14 (Figure 4D and E). The inhibition observed does not appear to be specific for either form of regulatory light chain because the

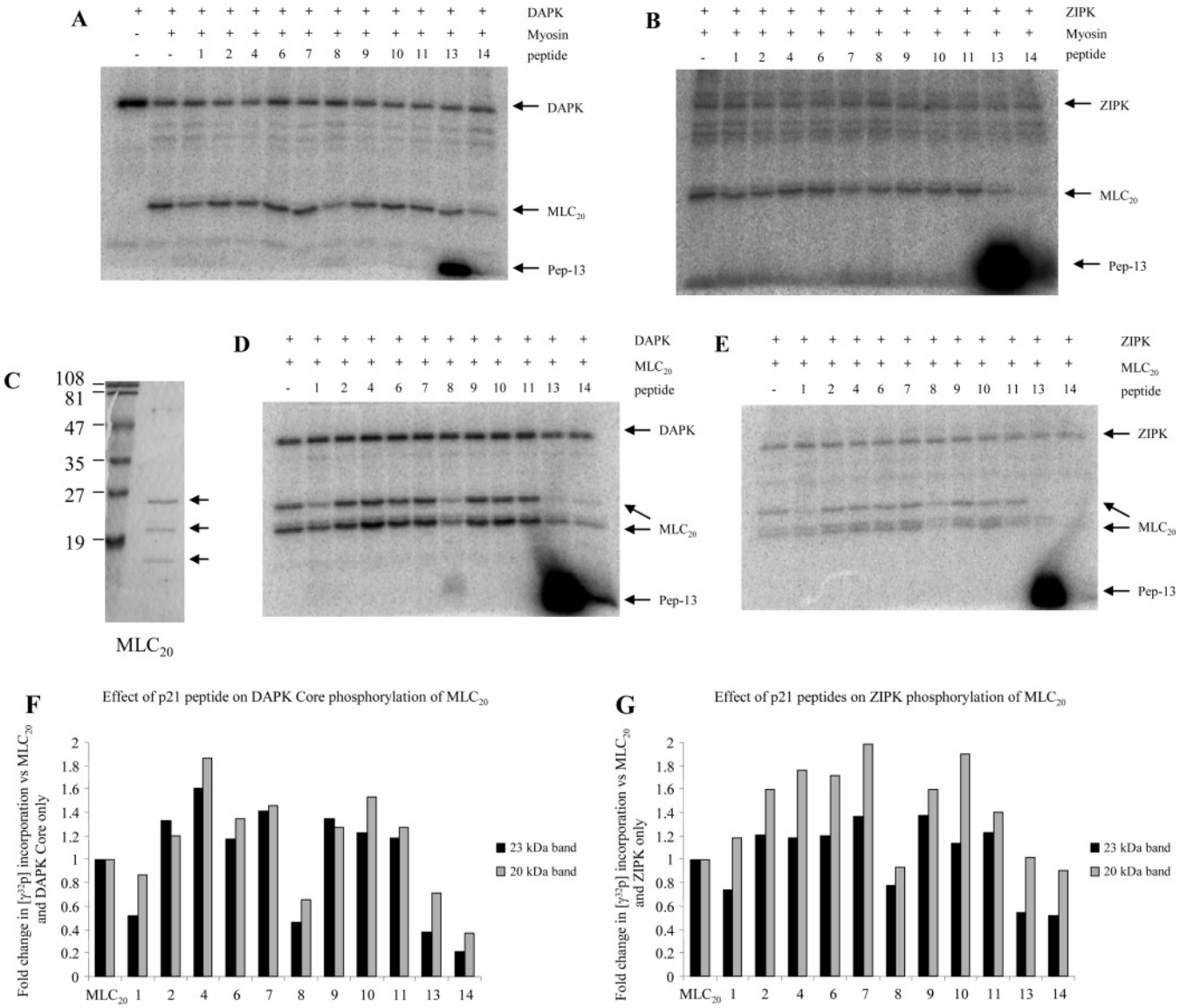


FIGURE 4: DAPK core and ZIPK activity toward myosin and $MLC_{20}$ is attenuated in the presence of p21 peptides. Kinase reactions containing [$\gamma^{32}$P]ATP, DAPK (A and D) or ZIPK (B and E), and either 1 $\mu$g of myosin (A and B) or 150 ng of $MLC_{20}$ (D and E) were assembled in the presence of the indicated p21 20-mer peptides. The samples were resolved by 12% SDS−PAGE, and reaction products were analyzed by autoradiography. (C) $MLC_{20}$ (150 ng) was resolved using 15% SDS−PAGE and stained with Coomassie blue. (F and G) The intensity of [$\gamma^{32}$P]ATP incorporation into $MLC_{20}$ bands was visualized by autoradiography, quantified by phosphorimager, and normalized to $MLC_{20}$ phosphorylation in the absence of the peptide.

quantification of [$\gamma^{32}$P]ATP incorporation by a phosphorimager shows the reduction observed was equivalent for both bands (Figure 4F and G). These findings demonstrate the ability to modulate the activity of DAPK family members toward weak or low-affinity substrates using synthetic peptides from high-affinity substrates. The fact that these peptides are not substrates for either DAPK or ZIPK suggests that the observed modification of activity may be an allosteric mechanism of action. An examination of the amino acid sequences of the stimulatory peptides does not reveal any striking similarity between the peptides (Figure 1C) or obvious repeat of sequence. These regions are not contiguous on p21; however, it is possible that these regions form some form of docking interface, which bind and potentially induce conformational changes to enhance basal activity toward the phospho-acceptor site.

To establish whether the increase in enzyme activity may be due to docking on the enzyme, we used ELISA to identify enzyme binding to p21 peptides. First, we captured GST-tagged DAPK core or ZIPK onto a 96-well plate via GST antibody and panned for binding peptides. The results of the ELISA mirrored those of the kinase assays with three regions of high-affinity peptide binding (Figure 5A and B): the N-terminal region (peptides 1, 2, 4, and 6; residues 1−65), the central region (peptide 10; residues 105−125), and the carboxyl terminal region (peptides 13 and 14; residues 135−164). Kinase assays showed that peptide 8 had the most striking stimulatory effect on DAPK core and ZIPK activity toward $p53^{1-66}$; however, peptide 8 did not show any binding by ELISA when DAPK core or ZIPK enzymes were bound to the plate by GST antibody (Figure 5A and B). This is possibly due to antibody capture disturbing or masking the region of peptide interaction because when the p21 peptides were bound to the plate using streptavidin, the weak binding of peptide 8 to DAPK core and ZIPK was observed (Figure 5C and D). Surprisingly, peptide 10 showed high-affinity

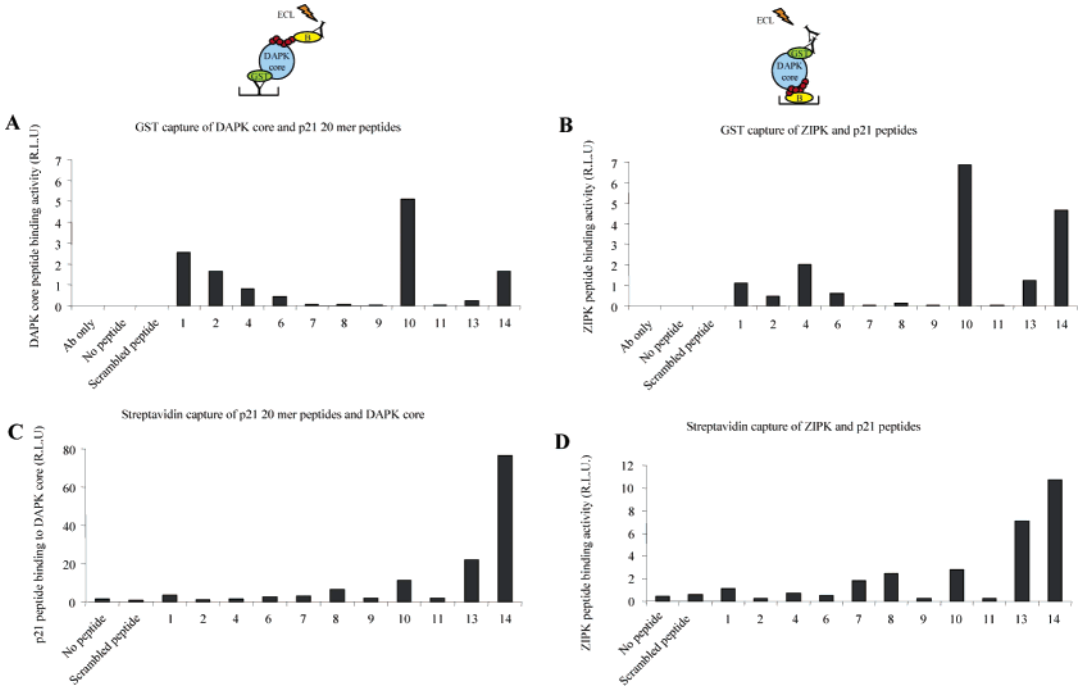


FIGURE 5: DAPK core and ZIPK bind specific regions of $p21^{WAF1}$. Direct binding of DAPK core (A and C) or ZIPK (B and D) to the p21 peptide was tested via ELISA using GST antibody capture of GST-tagged DAPK (A) or ZIPK (B), or streptavidin capture of biotinylated p21 peptides (C and D). The cartoons represent the mechanism of peptide capture.

ZIPK and DAPK core binding activity by ELISA; however, when peptide 10 was incubated with $p53^{1-66}$, no significant stimulation of DAPK core or ZIPK enzyme activity was observed (Figure 3C and D). If anything, utilization of $p53^{1-66}$ was inhibited in its presence. Slight inhibition of [$\gamma^{32}$P]ATP incorporation into $p53^{1-66}$ was also observed in the presence of peptides 2, 4, and 6, yet these peptides also demonstrate binding to DAPK core and ZIPK by ELISA (Figure 3C and D). These data demonstrate the power of combined ELISA and kinetic analyses for identifying the potential regions involved in enzyme−substrate interfaces and modulation of activity.

The ability of the p21 peptides to bind to and stimulate utilization of substrates with low-affinity consensus sites suggests that allosteric effects are involved in enzyme activity and may regulate substrate phosphorylation. To assess whether this may be due to a change in enzyme conformation, we used partial proteolytic mapping to establish whether any change in structure was occurring in the presence of the peptides. GST-tagged DAPK, full-length, and Core, and GST-tagged ZIPK were synthesized by *in vitro* transcription and translation (IVT) using rabbit reticulocyte lysates and labeled with L-[$^{35}$S] methionine. An analysis of the reaction products by SDS−PAGE and autoradiography revealed the presence of single bands corresponding to the expected full-length size of DAPK, DAPK core, and ZIPK protein products: ~160 kDa, ~57 kDa, and ~78 kDa respectively (Figure 6A). Partial digestion of the IVT DAPK forms with trypsin produced a major tryptic fragment of ~29 kDa for both full-length and core DAPK (Figure 6 B). ZIPK appears to be more sensitive to tryptic digestion because after 30 min on ice, the majority of full-length ZIPK had been digested, and a major tryptic fragment of ~32 kDa was apparent (Figure 6C). These data suggest that tryptic sensitive regions are exposed on the surface of DAPK and ZIPK. The ~29 and ~32 kDa tryptic bands were also observed when untagged forms of DAPK core and ZIPK generated by IVT were treated with trypsin (data not shown), indicating that these fragments are derived from DAPK and ZIPK and not from the GST tag. Inclusion of the stimulatory p21 peptides with DAPK (full length and core) or ZIPK in the presence of trypsin protected against proteolytic digestion of the full-length protein (Figure 6D, E, and F), as was seen by the increase in intensity of the full-length IVT products and a reduction in the presence of the major tryptic fragments. This was most apparent for peptide 14, which showed striking binding by ELISA (Figure 5) and completely prevented the formation of major ~29 and ~32 kDa DAPK and ZIPK tryptic bands (Figure 6D, E, and F). Peptide 1 also protected against digestion; however, in the presence of ZIPK protection, appeared to be more partial and was not as striking as that observed in the presence of peptide 14 (Figure 6F). Such protection from proteolytic digestion suggests that binding to peptides 1 and 14 may alter the conformation of DAPK and ZIPK such that the regions sensitive to trypsin are contorted or masked. Such changes may, therefore, be responsible for the observed increase in substrate utilization and enzyme activity seen in Figure 3.

To confirm that the effects of the p21 peptides were specific for DAPK and ZIPK and not due to the inhibition of trypsin, we tested the ability of the p21 peptides to protect $p53^{1-66}$ from proteolytic digestion. Partial digestion of $p53^{1-66}$ produced several tryptic fragments (Figure 6G). At low trypsin concentrations, a single tryptic fragment of approximately ~28 kDa was observed, whereas at higher trypsin concentrations, additional fragments of approximately ~27, 20, 15, 12, and 10 kDa were observed (Figure 6G). The intensity of these fragments were not altered by the presence of the stimulatory p21 peptides (Figure 6H), indicating that the peptides do not offer $p53^{1-66}$ any protection against tryptic digestion. Indeed, the digestion pattern of $p53^{1-66}$ observed in the presence of peptide 1 was

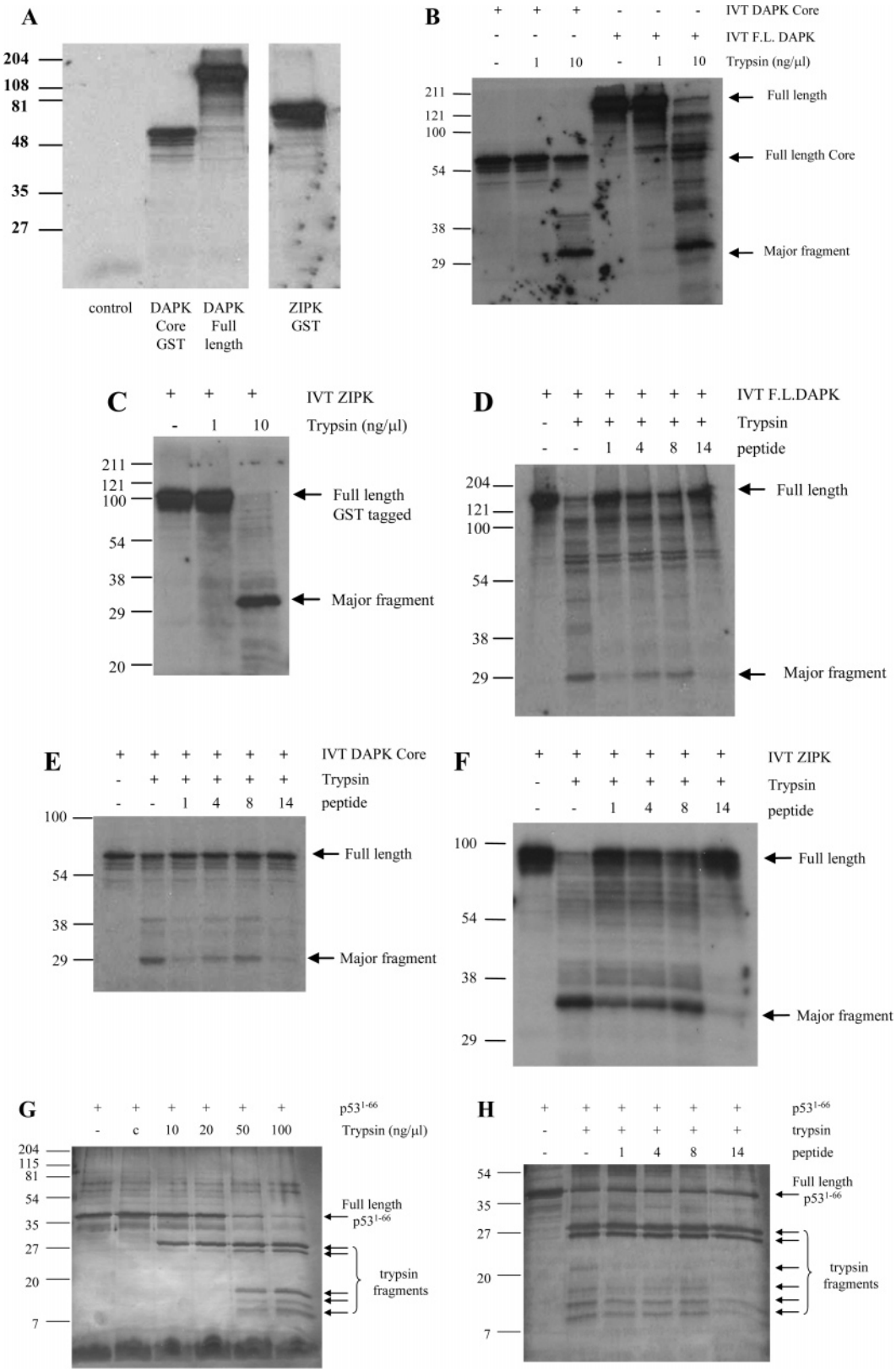


FIGURE 6: p21 stimulatory peptides protect DAPK and ZIPK against tryptic cleavage. (A) SDS−PAGE analyses of DAPK and ZIPK generated from reticulocyte lysate. DAPK core (lane 2), full-length DAPK (lane 3), and ZIPK (lane 4) were synthesized in reticulocyte lysate coupled transcription and translation and labeled with L-[$^{35}$S]methionine. The reaction products were resolved by 12% SDS−PAGE and visualized by autoradiography. (B and C) Tryptic digestion of DAPK and ZIPK. The reactions containing L-[$^{35}$S] labeled *in vitro* translated (IVT) DAPK and full-length and core (B) and ZIPK (C) were assembled in the presence of 1 or 10 ng of trypsin and incubated on ice for 30 min. Tryptic fragments were resolved by SDS−PAGE and visualized by autoradiography. (D, E, and F) p21 peptides protect DAPK and ZIPK from tryptic cleavage. The reactions containing IVT GST-tagged DAPK, full-length (D) DAPK core (E), or ZIPK (F) were assembled with the indicated p21 peptides in the presence of 10 ng/mL trypsin on ice for 30 min and analyzed as above. (G and H) Tryptic digestion of GST-tagged p53$^{1-66}$. (G) Reactions containing 300 ng of p53$^{1-66}$ and the indicated concentration of trypsin were assembled and incubated on ice for 30 min. Tryptic fragments were resolved by 15% SDS−PAGE and detected using silver staining. (H) Reactions containing p53$^{1-66}$, 50 ng/$\mu$L trypsin, and the indicated p21 peptide were assembled and analyzed as in (G).

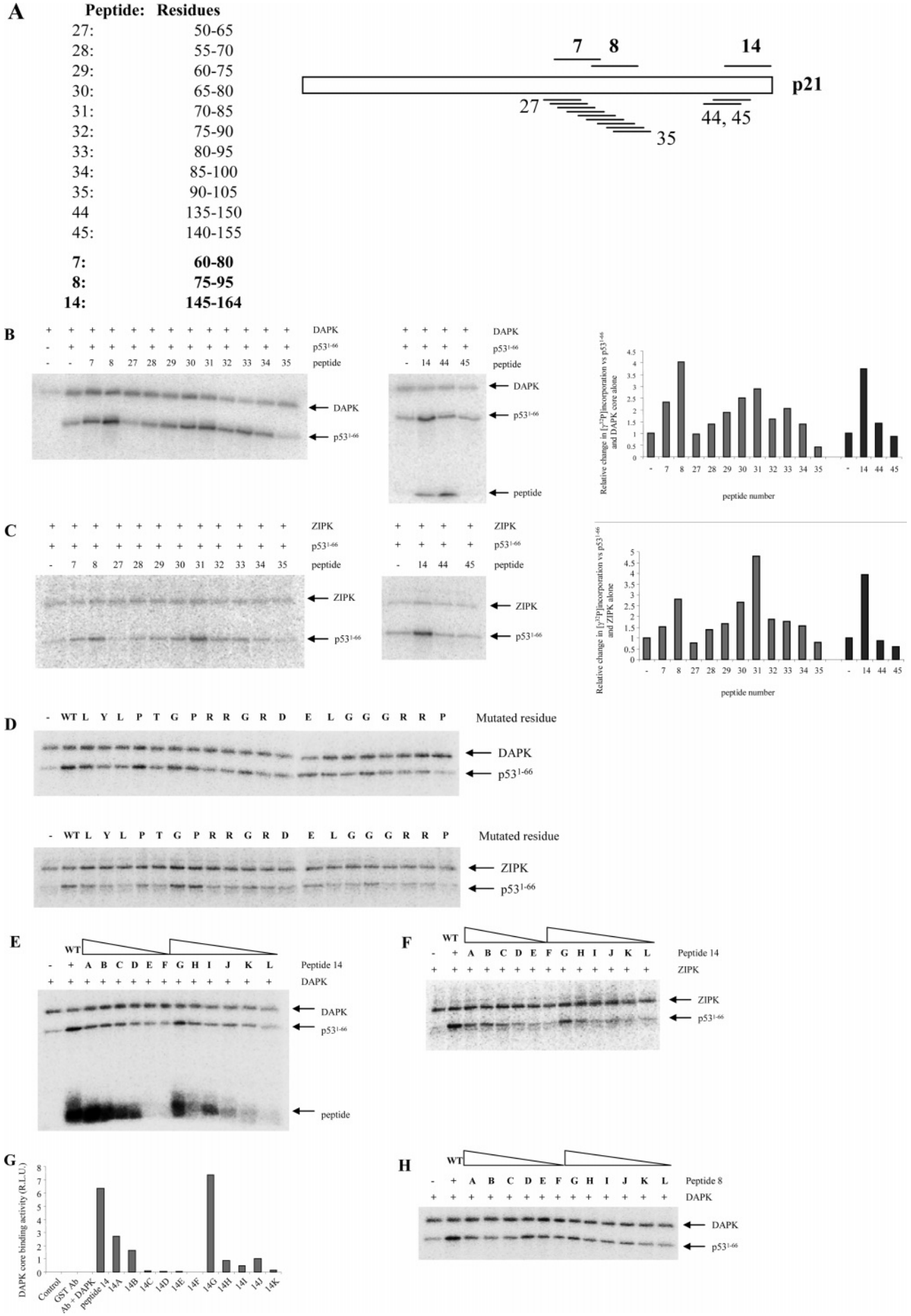
A
Peptide: Residues
27: 50-65
28: 55-70
29: 60-75
30: 65-80
31: 70-85
32: 75-90
33: 80-95
34: 85-100
35: 90-105
44 135-150
45: 140-155
7: 60-80
8: 75-95
14: 145-164
7 8 14
p21
27
35
44, 45
B
DAPK
p53 1-66
peptide
Relative change in [γ-32P]incorporation vs p53 1-66 and DAPK core alone
peptide number
C
ZIPK
p53 1-66
peptide
Relative change in [γ-32P]incorporation vs p53 1-66 and ZIPK alone
peptide number
D
- WT L Y L P T G P R R G R D E L G G G R R P
Mutated residue
DAPK
p53 1-66
ZIPK
E
WT
Peptide 14
DAPK
peptide
F
WT
Peptide 14
ZIPK
G
DAPK core binding activity (R.L.U.)
Control
GST Ab
Ab + DAPK
peptide 14
14A
14B
14C
14D
14E
14F
14G
14H
14I
14J
14K
H
WT
Peptide 8
DAPK

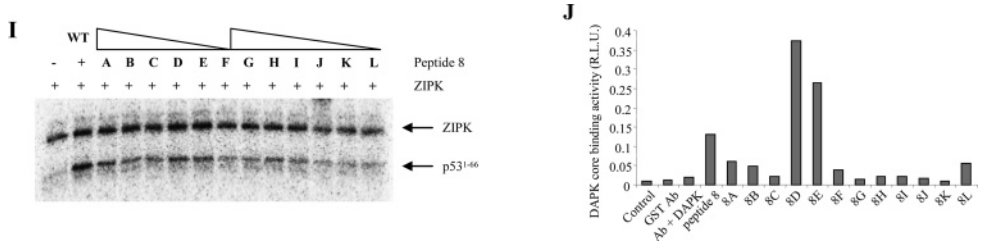


FIGURE 7: Fine mapping of the regions of p21 peptides that stimulate $p53^{1-66}$ activity. (A) Synthetic p21 15-mer peptides overlapping the regions of peptides 8 and 14 were synthesized and analyzed for their ability to stimulate DAPK core and ZIPK activity. The cartoon depicts the regions covered by the peptides. The kinase reactions containing DAPK core (B) or ZIPK (C), [$\gamma^{32}$P]ATP, 150 ng of $p53^{1-66}$, and the indicated overlapping p21 15-mer peptides (final concentration ~50 $\mu$M) were assembled. Samples were resolved by 12% SDS−PAGE, and reaction products were analyzed by autoradiography. [$\gamma^{32}$P]ATP incorporation into $p53^{1-66}$ by DAPK and ZIPK was quantified by a phosphorimager. (D) Mutation of peptide 8 attenutates its ability to stimulate DAPK core and ZIPK. The reactions containing DAPK core (upper panel) or ZIPK (lower panel), [$\gamma^{32}$P]ATP, 150 ng of $p53^{1-66}$, and peptides containing alanine-scan mutations in peptide 8 were assembled and analyzed as in (B). (E and F) Truncation of peptide 14 attenuates its ability to stimulate DAPK core and ZIPK. The reactions were assembled as in (B) with the indicated truncation of peptide 14 and analyzed as in (B). (G) Truncation of peptide 14 attenuates its ability to bind DAPK core. DAPK core was captured by GST antibody, and binding of the peptide 14 truncations was determined by ELISA. (H and I) Truncation of peptide 8 attenuates its ability to stimulate DAPK core and ZIPK. The reactions containing the indicated truncation of peptide 8 were assembled and analyzed as in (B). (J) Truncation of peptide 8 attenuates binding to DAPK core. Binding of the peptide 8 truncations to DAPK core was determined by ELISA.

identical to that of peptide 4 (Figure 6H). This is in contrast to the findings for DAPK and ZIPK, where peptide 1 protected DAPK and ZIPK against tryptic cleavage, whereas peptide 4 offered limited protection (Figure 6D, E, and F). These findings, therefore, suggest that the p21 peptides are unable to bind to and alter the conformation of $p53^{1-66}$, thereby preventing tryptic cleavage, and show that the protective effect of the peptides is specific for DAPK and ZIPK. They also indicate that the modulatory effects of the p21 peptides are due to binding and modification of DAPK and ZIPK conformation and activity rather than peptide binding to p53 creating a better DAPK and ZIPK substrate. Indeed, had the p21 peptides mediated their modulatory effects through substrate interaction, $MLC_{20}$ utilization by DAPK and ZIPK would also have been enhanced in their presence. These findings thus support the hypothesis that interaction with the peptides switches the conformation of DAPK and ZIPK.

A slight decrease in intensity of the 20, 15, 12, and 10 kDa tryptic fragments was observed when $p53^{1-66}$ was digested in the presence of peptide 14 (Figure 6H). Be cause peptide 14 has a number of lysine residues within its structure, this may be due to slight competition between peptide 14 and $p53^{1-66}$ for digestion. However, the protection conferred upon DAPK and ZIPK by peptide 14 (Figure 6D, E, and F) was far more striking than the protection offered to $p53^{1-66}$ (Figure 6H), suggesting that inhibition of tryptic activity alone was not responsible for the protection offered by peptide 14 and that additional conformational changes must have been involved.

Peptide 8 was able to stimulate DAPK core and ZIPK activity (Figure 3A and B); however, it was unable to protect IVT DAPK and ZIPK from proteolytic cleavage, and the intensity of the major tryptic band was comparable to that of the control (Figure 6D, E, and F). Indeed, in the presence of peptide 8, the tryptic profile was more akin to that obtained in the presence of peptide 4, which was used as a control because of its lack of stimulatory ability toward DAPK core and ZIPK (Figure 3). These findings suggest that interaction with peptide 8 may not induce a dramatic conformational change such as that of peptide 1 and 14. Alternatively, it is possible that the on−off rate of peptide binding is so rapid that it is unable to protect against tryptic cleavage. It does not, however, rule out the possibility that association with peptide 8 enhances DAPK core and ZIPK activity toward $p53^{1-66}$ by promoting substrate binding and utilization in the absence of any major structural changes.

In an attempt to refine the regions and residues important for the activation of via the potential docking interface, we generated synthetic 15-mer p21 peptides, which overlap the regions corresponding to peptides 7, 8, and 14 and residues 60−95 (peptides 7 and 8) and 145−164 (peptide 14) (Figure 7A). The use of these peptides permits gross analysis of structure by removing five amino acid residue chunks at a time. Peptides 28−34 enhance DAPK core activity toward $p53^{1-66}$ above control levels (Figure 7B); however. neither peptide 27 nor peptide 35, corresponding to residues 50−65 and 90−105, respectively, was able to enhance $p53^{1-66}$ utilization by DAPK core. Because peptides 7 and 8 cover residues 60−80 and 75−95, this suggests that residues 60−65 and 90−95 are not essential for the observed peptide-induced increase in DAPK core activity. Although peptides 28−34 were able to stimulate DAPK core activity, only peptides 30 and 31 were able to recapitulate the degree of stimulation observed in the presence of peptide 7, suggesting that residues 70−80 are important for the activation of DAPK core. Peptide 8 afforded an ~4-fold increase in [$\gamma^{32}$P]ATP incorporation into $p53^{1-66}$ by DAPK core; however, none of the overlapping 15-mer peptides used here were able to generate the same degree of stimulation (Figure 7B). This suggests that the gross truncation of peptide 8 disrupts the binding interface with DAPK core and attenuates its stimulatory activity. In contrast to DAPK core, peptide 28 was unable to enhance ZIPK activity toward $p53^{1-66}$ above control levels (Figure 7C), and only peptides 29−34 were able to potentiate ZIPK activity, suggesting that residues 60−70 and 90−95 are not essential for the observed increase in ZIPK activity. Furthermore, peptides 30 and 31 were not only able to stimulate ZIPK activity toward $p53^{1-66}$, but the degree of [$\gamma^{32}$P]ATP incorporation into $p53^{1-66}$ was comparable to that of peptide 8 (Figure 7C). This indicates that although peptide 8 is capable of activating both DAPK core and ZIPK activity, subtle differences exist between the precise interface formed between the two enzymes and peptide 8 to generate activation.

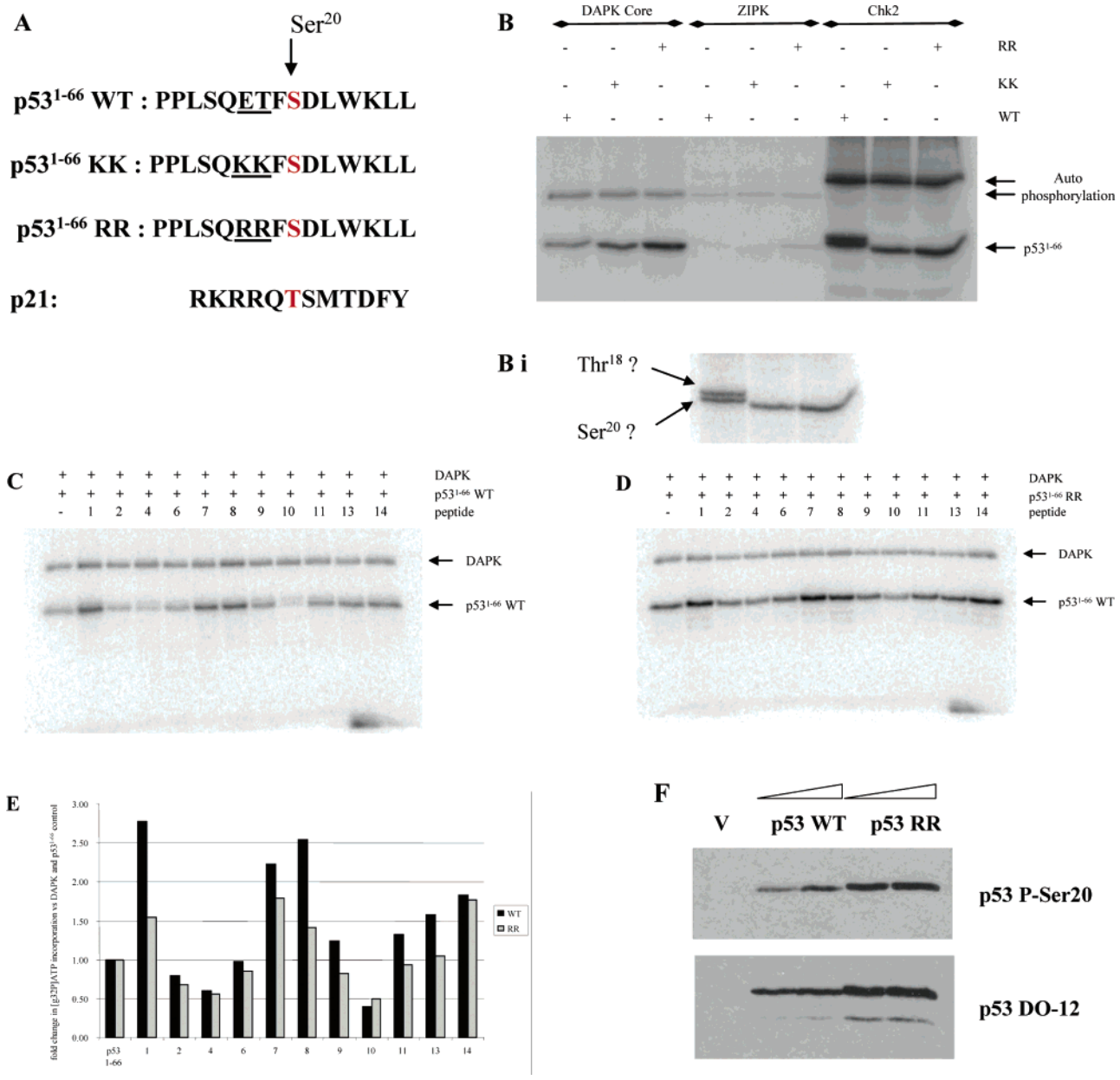


FIGURE 8: Mutation of the $p53^{1-66}$ consensus site enhances $p53^{1-66}$ utilization by DAPK core and ZIPK. (A) Indication of the mutations generated around the $p53^{1-66}$ $Ser^{20}$ phosphorylation site. (B) Analysis of $p53^{1-66}$ mutant utilization by DAPK, ZIPK, and Chk2. The kinase reactions containing [$\gamma^{32}$P]ATP, 150 ng of $p53^{1-66}$, $p53^{1-66[ET\rightarrow KK]}$, or $p53^{1-66[ET\rightarrow RR]}$ were assembled in the presence of DAPK, ZIPK ,and Chk2, resolved by 12% SDS−PAGE, and analyzed by autoradiography. (B i) Lower exposure of [$\gamma^{32}$P]ATP incorporation into $p53^{1-66}$, $p53^{1-66[ET\rightarrow KK]}$, and $p53^{1-66[ET\rightarrow RR]}$ by Chk2. (C and D) Effect of $p53^{1-66[ET\rightarrow RR]}$ mutation on p21 peptides ability to stimulate DAPK core activity. The kinase reactions containing [$\gamma^{32}$P]ATP, DAPK, and 150 ng of wild type or $p53^{1-66[ET\rightarrow RR]}$ were assembled in the presence of p21 20-mer peptides and further resolved using 12% SDS−PAGE, and the intensity of [$\gamma^{32}$P]ATP incorporation into $p53^{1-66}$ was visualized by autoradiography and quantified by a phosphorimager (E). (F) Mutation of $p53^{[E17I18\rightarrow R17R18]}$ enhances $Ser^{20}$ phosphorylation *in vivo*. H1299 cells were transiently transfected with 1 $\mu$g of pcDNA3.1 (V) or 0.5 or 1 $\mu$g of pcDNA3.1 $p53^{1-66}$WT or the $p53^{1-66[ET\rightarrow RR]}$ mutant. Twenty-four hours later, cells were harvested, and P-$Ser^{20}$ (upper panel) and whole p53 levels (lower panel) were determined by Western blotting.

To clarify this, the effect of individual amino acid mutations on peptide 8 activation of DAPK core and ZIPK were examined (Table 1). The mutation of residues to alanine at positions $Arg^{82}$, $Arg^{85}$, $Asp^{86}$, $Leu^{88}$, $Gly^{89}$, $Gly^{91}$, $Arg^{92}$, $Arg^{93}$, and $Pro^{94}$ attenuated DAPK core activation by peptide 8 (Figure 7D), whereas ZIPK activation by peptide 8 was attenuated by alanine substitution at positions $Leu^{77}$, $Arg^{82}$, $Leu^{88}$, $Gly^{89}$, $Gly^{91}$, $Arg^{92}$, $Arg^{93}$, and $Pro^{94}$ (Figure 7D). In contrast, alanine mutation at $Gly^{80}$ and $Pro^{81}$ slightly enhanced peptide 8 activation of ZIPK activity. These findings suggest that residues at the COOH terminal of peptide 8 are responsible for activating both DAPK and ZIPK, whereas selectivity between the activation of DAPK core or ZIPK is conferred by residues at the $NH_2$ terminal of peptide 8.

Peptides 44 and 45 contain the amino acid residues covered by peptide 14 (residues 145−164); however, neither peptide was able to generate any increase in [$\gamma^{32}$P]ATP incorporation into $p53^{1-66}$ by DAPK core or ZIPK above back ground levels (Figure 7B and C). Indeed, peptides 44 and 45 were not even able to partially stimulate enzyme activity. These findings suggest that the peptide 14 binding interface is large

Table 1: Indication of the Positioning of Alanine Mutations Made within Peptide 8

| Peptide 8 Alanine scan: | Sequence |
|---|---|
| Ala 1 (L75A): | **A**YLPTGPRRGRDELGGGRRP |
| Ala 2 (Y76A): | L**A**LPTGPRRGRDELGGGRRP |
| Ala 3 (L77A): | LY**A**PTGPRRGRDELGGGRRP |
| Ala 4 (P78A): | LYL**A**TGPRRGRDELGGGRRP |
| Ala 5 (T79A): | LYLP**A**GPRRGRDELGGGRRP |
| Ala 6 (G80A): | LYLPT**A**PRRGRDELGGGRRP |
| Ala 7 (P81A): | LYLPTG**A**RRGRDELGGGRRP |
| Ala 8 (R82A): | LYLPTGP**A**RGRDELGGGRRP |
| Ala 9 (R83A): | LYLPTGPR**A**GRDELGGGRRP |
| Ala 10 (G84A): | LYLPTGPRR**A**RDELGGGRRP |
| Ala 11 (R85A): | LYLPTGPRRG**A**DELGGGRRP |
| Ala 12 (D86A): | LYLPTGPRRGR**A**ELGGGRRP |
| Ala 13 (E87A): | LYLPTGPRRGRD**A**LGGGRRP |
| Ala 14 (L88A): | LYLPTGPRRGRDE**A**GGGRRP |
| Ala 15 (G89A): | LYLPTGPRRGRDEL**A**GGRRP |
| Ala 16 (G90A): | LYLPTGPRRGRDELG**A**GRRP |
| Ala 17 (G91A): | LYLPTGPRRGRDELGG**A**RRP |
| Ala 18 (R92A): | LYLPTGPRRGRDELGGG**A**RP |
| Ala 19 (R93A): | LYLPTGPRRGRDELGGGR**A**P |
| Ala 20 (P94A): | LYLPTGPRRGRDELGGGRR**A** |

and complex and that gross truncation around this region critically perturbs its stimulatory capacity.

Because gross deletion around the regions of peptides 8 and 14 severely disrupts their ability to stimulate DAPK core and ZIPK activity, we generated smaller amino acid deletions within peptides 8 and 14 to try to map the core regions required for stimulation (Table 2). The truncation of peptide 14 drastically reduced its stimulatory capacity and compromised its ability to stimulate DAPK core activity toward $p53^{1-66}$ (Figure 7E). Indeed, there was a strong correlation between the extent of peptide 14 truncation and its ability to stimulate DAPK core phosphorylation of $p53^{1-66}$. The loss of peptide 14 stimulation because of N- and C-terminal truncation was also apparent when peptides 14 A−14 L were analyzed with ZIPK (Figure 7F), and a similar, if not more dramatic loss of stimulation by peptide 14 toward ZIPK was observed. The removal of residues 75−82 and 88−95 (Figure 7E and F, compare full length with peptides 14 F and 14 L, respectively) completely prevented the stimulation of both DAPK core and ZIPK activity toward $p53^{1-66}$, suggesting that the central core of peptide 14 (residues 82−88) is not responsible for the stimulation of activity. The loss of peptide 14 stimulatory capacity also correlated with the loss of peptide binding to DAPK core (Figure 7G). The binding activity of peptide 14 A to DAPK core was half that observed in the presence of full-length peptide 14, whereas peptide 14 B retained only 30% binding activity of full-length peptide 14. Peptides 14 C, D, E, and F showed no binding activity. Binding of peptide 14 G was comparable to that of full-length peptide 14; however, clipping of the residues at the $NH_2$ terminal (peptides 14 H−14 L) dramatically reduced binding to DAPK core. These findings illustrate that residues at both ends of peptide 14 are important for both binding and stimulation of DAPK and ZIPK activity toward $p53^{1-66}$, suggesting that peptide 14 must form a large binding interface with both DAPK core ZIPK. More in-depth structural analyses will, however, be required to confirm this.

Truncation of residues from the $NH_2$ terminal of peptide 8 also reduced its ability to stimulate DAPK core activity. Clipping of residues from the COOH terminal of peptide 8 was sufficient to prevent the stimulation of DAPK core activity observed with full-length peptide 8 because DAPK core activity toward $p53^{1-66}$ phosphorylation in the presence of peptides 8 A, 8 B, and 8 C was comparable to that of the control levels (Figure 7H). The removal of residues from the $NH_2$ terminal of peptide 8 also abrogated the stimulation of DAPK core by peptide 8. Although peptide 8 G was able to stimulate DAPK core activity to a degree comparable to that of full-length peptide 8 $p53^{1-66}$, peptides 8 H−L were unable to generate any stimulation, and [$\gamma^{32}$P] ATP incorporation into $p53^{1-66}$ was comparable to that of DAPK alone (Figure 7H). A similar profile of stimulation by truncated peptide 8 was also observed in the presence of ZIPK (Figure 7I). Surprisingly, the phosphorylation of $p53^{1-66}$ by DAPK core in the presence of peptide 8 D and E was more comparable to that of DAPK core plus full-length peptide 8. This was also observed when ZIPK was incubated with peptide 8 D and E. Analyses of peptide 8 binding by ELISA shows that peptide 8 D and E bound to DAPK core more strongly than full-length peptide 8 (Figure 7J). These findings suggest that the regions of peptide 8 between residues 88 and 93 may be inhibitory because the stimulation of DAPK core activity in their presence is prevented. Alternatively, it is possible that peptide 8 has a precise secondary structure, and specific truncations (i.e., A, B, and C) may effect peptide conformation such that binding and activation is impinged.

Increasing the basic nature of the region downstream of the consensus phosphorylation site by addition of lysine residues enhances peptide−substrate utilization by DAPK (*11*). We wanted to see whether modification of the $p53^{1-66}$ consensus phosphorylation region to be more like that of efficiently utilized substrates such as p21 could promote $p53^{1-66}$ utilization by DAPK core. To test this, we introduced basic lysine and arginine mutations into $p53^{1-66}$, N-terminal of the $Ser^{20}$ phospho-acceptor site at $Glu^{17}$ and $Thr^{18}$ (Figure 8A). The positioning of the mutations was based on the location of basic residues in the consensus site of p21, the best DAPK core and ZIPK substrate tested in this study (Figure 2A). When equal concentrations of $p53^{1-66}$ wild type and mutants were incubated with DAPK core and ZIPK, phosphorylation of the mutant p53 forms was greater than that of wild-type $p53^{1-66}$ (Figure 8B). Quantification of [$\gamma^{32}$P]-ATP incorporation into $p53^{1-66}$ by DAPK using the phosphorimager showed an ~1.5- and 2.5-fold increase in $p53^{1-66[ET\rightarrow KK]}$ and $p53^{1-66[ET\rightarrow RR]}$ phosphorylation compared to that of wild-type $p53^{1-66}$, whereas in the presence of ZIPK, [$\gamma^{32}$P]ATP incorporation into $p53^{1-66[ET\rightarrow KK]}$ and $p53^{1-66[ET\rightarrow RR]}$ was ~1.2- and 4.2-fold greater than that of the wild type. Increasing the basic nature of the N-terminal region of p53 $Ser^{20}$ consensus site, therefore, improves $p53^{1-66}$ utilization by DAPK core and ZIPK.

In contrast, Chk2 showed very little change in activity toward the $p53^{1-66}$ mutants. Two distinct $p53^{1-66}$ bands corresponding to phosphorylated p53 are observed in the presence of Chk2 (Figure 8B i). Previous analyses using phospho-specific antisera suggested that the upper band may correspond to the phosphorylation of $p53^{1-66}$ at $Thr^{18}$ (possibly also dual phosphorylation at $Thr^{18}$/$Ser^{20}$), whereas the lower band corresponds to phosphorylation at $Ser^{20}$ (*9*).

Table 2: List of Peptide Truncations Made to p21 Peptides 8 and 14

| Peptide 8 | Sequence | Peptide 14 | Sequence |
|---|---|---|---|
| **WT:** | **LYLPTGPRRGRDELGGGRRP** | **WT:** | **TSMTDFYHSKRRLIFSKRKP** |
| **A** | LYLPTGPRRGRDELGGGR | **A** | TSMTDFYHSKRRLIFSKR |
| **B** | LYLPTGPRRGRDELGG | **B** | TSMTDFYHSKRRLIFS |
| **C** | LYLPTGPRRGRDEL | **C** | TSMTDFYHSKRRLI |
| **D** | LYLPTGPRRGRD | **D** | TSMTDFYHSKRR |
| **E** | LYLPTGPRRG | **E** | TSMTDFYHSK |
| **F** | LYLPTGPR | **F** | TSMTDFYH |
| **G** | LPTGPRRGRDELGGGRRP | **G** | MTDFYHSKRRLIFSKRKP |
| **H** | TGPRRGRDELGGGRRP | **H** | DFYHSKRRLIFSKRKP |
| **I** | PRRGRDELGGGRRP | **I** | YHSKRRLIFSKRKP |
| **J** | RGRDELGGGRRP | **J** | SKRRLIFSKRKP |
| **K** | RDELGGGRRP | **K** | RRLIFSKRKP |
| **L** | ELGGGRRP | **L** | LIFSKRKP |

Table 3: Kinetic Constants for DAPK core with Respect to $p53^{1-66}$ Mutants

| | $K_m$ $\mu$M | $V_{max}$ pCi/min/mg DAPK | $k_{cat}$ $min^{-1}$ | $k_{cat}/K_m$ $min^{-1}\,\mu m^{-1}$ |
|---|---|---|---|---|
| $p53^{1}$-66WT | 0.57 ± 0.08 | 5.61 ± 2.24 | 325.37 ± 129.81 | 600.16 ± 323.34 |
| $p53^{1}$-66KK | 1.59 ± 0.05 | 10.44 ± 2.68 | 605.45 ± 155.44 | 383.11 ± 109.21 |
| $p53^{1}$-66RR | 10.81 ± 1.66 | 244.10 ± 5.80 | 14150.72 ± 336.13 | 1327.20 ± 234.53 |

Table 4: Kinetic Constants for DAPK core with Respect to ATP in the Presence of $p53^{1-66}$ Mutants

| | $K_m$ $\mu$M | $V_{max}$ pCi/min/mg | $k_{cat}$ $min^{-1}$ | $k_{cat}/K_m$ $min^{-1}\,\mu m^{-1}$ |
|---|---|---|---|---|
| $p53^{1-66}$WT | 1.71 ± 0.77 | 5.31 ± 2.04 | 308.03 ± 118.10 | 183.18 ± 13.50 |
| $p53^{1-66}$RR | 5.32 ± 1.44 | 63.95 ± 14 89 | 3707.25 ± 863. 29 | 700.25 ± 27.49 |

Findings in this study support this suggestion because the upper band was lost in the lanes containing $p53^{1-66[ET\rightarrow KK]}$ and $p53^{1-66[ET\rightarrow RR]}$ in which the $Thr^{18}$ site is mutated (Figure 8B). In the presence of DAPK core and ZIPK, only one band corresponding to $p53^{1-66}$ is observed, suggesting that both DAPK core and ZIPK only modify $p53^{1-66}$ at $Ser^{20}$. Quantification suggests that Chk2 phosphorylation at $Ser^{20}$ is not greatly effected by the presence of KK and RR residues downstream of the phospho-acceptor site because [$\gamma^{32}$P]ATP incorporation into the lower P-$Ser^{20}$ band of $p53^{1-66[ET\rightarrow KK]}$ and $p53^{1-66[ET\rightarrow RR]}$ mutants was 0.84- and 1.34-fold that of wild-type $p53^{1-66}$, respectively. These finding suggest the mutations made $p53^{1-66}$ a better substrate for DAPK and ZIPK without effecting utilization by other kinases such as Chk2.

To confirm that the $p53^{1-66}$ mutants were more effectively used than the wild-type $p53^{1-66}$ by DAPK core, we analyzed the kinetics of $p53^{1-66}$ use. Concentrations of wild-type and KK mutant $p53^{1-66}$ ranging from 0.02 to 2.48 $\mu$M were used to calculate the apparent $K_m$ and $V_{max}$ values (Table 3) and were sufficient to obtain the saturation of DAPK core activity and an apparent $V_{max}$. In contrast, saturation of DAPK core activity was not achieved when similar concentrations of the $p53^{1-66[ET\rightarrow RR]}$ mutant were used. The highest concentration of $p53^{1-66[ET\rightarrow RR]}$ we were able to use in our reactions was 10.33 $\mu$M, yet even this was insufficient to saturate enzyme activity, and DAPK activity toward $p53^{1-66[ET\rightarrow RR]}$ was still in the linear range. We were, however, able to generate kinetic estimates from the values obtained using such concentration ranges. When $p53^{1-66[ET\rightarrow KK]}$ was used as a substrate, the apparent $V_{max}$ was ~2-fold greater than that of wild-type $p53^{1-66}$, whereas the apparent $V_{max}$ for $p53^{1-66[ET\rightarrow RR]}$ was ~40-fold greater than that of the wild type and ~20-fold greater than that of $p53^{1-66}$ KK (Table 3). In contrast, the addition of basic mutations at $Glu^{17}$ and $Thr^{18}$ reduced the apparent $K_m$ for $p53^{1-66}$, and the values for wild-type $p53^{1-66}$, $p53^{1-66[ET\rightarrow KK]}$, and $p53^{1-66[ET\rightarrow RR]}$ were 0.57, 1.59, and 10.81 $\mu$M, respectively. The $k_{cat}/K_m$ value for DAPK core in the presence of $p53^{1-66[ET\rightarrow RR]}$ was significantly higher than that of wild-type $p53^{1-66}$ (Table 3), suggesting that DAPK core is catalytically more efficient in the presence of mutant $p53^{1-66}$.

To determine whether the change in catalytic efficiency was due solely to p53 use, the $K_m$ and $V_{max}$ values for ATP in the presence of wild-type and RR mutant $p53^{1-66}$ were calculated. The apparent $K_m$ for DAPK core and ATP using wild-type $p53^{1-66}$ was found to be 1.71 $\mu$M, similar to the value of 2.4 $\mu$M reported previously (*11*). Surprisingly, in the presence of $p53^{1-66[ET\rightarrow RR]}$, the apparent $K_m$ for ATP increased from 1.71 to 5.32 $\mu$M (Table 4). There was also a ~12-fold increase in the apparent $V_{max}$ and $k_{cat}$ in the presence of $p53^{1-66[ET\rightarrow RR]}$ compared to those of wild-type $p53^{1-66}$. The $k_{cat}/K_m$ value for ATP in the presence of $p53^{1-66[ET\rightarrow RR]}$ was also significantly higher than that of wild-type $p53^{1-66}$ (Table 4), suggesting that the efficiency of ATP utilization by DAPK core is enhanced in the presence of mutant $p53^{1-66}$. These findings highlight the importance of residues in and around the phospho-acceptor site in influencing efficient substrate utilization and the potential interactions between ATP and $p53^{1-66}$ at the active site of DAPK core.

To test whether DAPK core activity toward $p53^{1-66[ET\rightarrow RR]}$ could be further stimulated, we analyzed $p53^{1-66[ET\rightarrow RR]}$ utilization in the presence of the p21 docking peptides. Surprisingly, p21 peptides were still able to stimulate DAPK core activity toward $p53^{1-66[ET\rightarrow RR]}$, and increased [$\gamma^{32}$P]ATP incorporation into $p53^{1-66[ET\rightarrow RR]}$ was observed in the presence of peptides 1, 7, 8, and 14 (Figure 8 D). Indeed, in spite of the increase basal level of $p53^{1-66[ET\rightarrow RR]}$ phosphorylation, the profile of stimulation obtained was similar to that of wild-type $p53^{1-66}$ (Figure 8C). The degree of [$\gamma^{32}$P]-ATP incorporation into wild-type and RR mutant $p53^{1-66}$ by DAPK was quantified by phosphorimager, and the fold change in phosphorylation was normalized to $p53^{1-66}$ phosphorylation in the absence of peptides (Figure 8E). The extent of the stimulation of DAPK core activity observed in the presence of peptide 14 for $p53^{1-66[ET\rightarrow RR]}$ was comparable to that of wild-type $p53^{1-66}$; however, the degree of DAPK stimulation afforded by peptides 1 and 8 in the presence of $p53^{1-66[ET\rightarrow RR]}$ was almost half of that observed when wild-type $p53^{1-66}$ was used as a substrate. These findings suggest that binding by peptide 1 and 8 may induce conformational changes within DAPK core, which promotes substrate binding at the active site and improves substrate utilization. For $p53^{1-66[ET\rightarrow RR]}$, the increased basic nature of the consensus site may enhance its interaction with residues around the substrate binding pocket promoting substrate phosphorylation, thus reducing the requirement for further conformational changes to create efficient interaction and phosphorylation. Peptide 14, however, may stimulate enzyme activity in a manor that is independent of increased $p53^{1-66}$ binding.

To examine whether the mutation of the p53 consensus site would also enhance full-length p53 utilization by a kinase to induce $Ser^{20}$ phosphorylation *in vivo*, we transfected H1299 cells, which are p53 null, with full-length p53 WT and $p53^{E17T18\rightarrow R17R18}$ constructs. Western blotting showed that the $Ser^{20}$ levels in cells transfected with $p53^{E17T18\rightarrow R17R18}$ were almost twice as high as that of p53 WT (Figure 8F), demonstrating that an ET−RR change in p53 can make full-length p53 a better substrate for an *in vivo* $Ser^{20}$ kinase. The increase in $Ser^{20}$ phosphorylation was also accompanied by an increase in the whole cell levels of p53 (Figure 8F). This observation was reproducible, and because cells were transfected with equal concentrations of plasmid DNA, it is thought that this represents stabilization of p53 because modification and phosphorylation of $Ser^{20}$ is known to perturb p53 interaction with Mdm2 interaction and promote interaction with p300, thus stabilizing steady-state levels of p53 (*25*, *26*). These findings show that the ET−RR mutation of the DAPK consensus phosphorylation site of p53 not only enhances substrate utilization *in vitro* but also influences the stability of full-length p53 *in vivo*.

## DISCUSSION

DAPK is a large multidomain protein known to cause cell death in response to several apoptotic signals. Like other members of the calmodulin (CaM) kinase superfamily, DAPK activity is regulated by the binding of CaM to the CaM binding domain, and the deletion of the CaM domain generates a constitutively active kinase with far greater killing potential *in vivo* (*27*). In the absence of apoptotic stimulus, the CaM binding domain binds to the catalytic cleft as a pseudo substrate, blocking substrate access and suppressing catalytic activity. The CaM binding domain also undergoes autophosphorylation at $Ser^{308}$, which further inhibits enzyme activity by reducing the binding affinity for CaM and stabilizing the pseudosubstrate interaction (*28*). Activation of DAPK, therefore, requires $Ca^{2+}$CaM binding to the CaM binding motif and dephosphorylation of $Ser^{308}$ by an as yet unidentified phosphatase. Dephosphorylation of $Ser^{308}$ alone increases CaM binding affinity, promotes DAPK activity at low $Ca^{2+}$CaM concentrations (*28*), and has been observed *in vivo* in response to several forms of apoptotic stimuli including TNFα, cerebral ischemeia (*15*) and unliganded dependence receptors (*29*). Few mechanisms for regulating DAPK activity out with the CaM binding domain have been described. In this study, we show that DAPK activity toward certain substrates can be regulated allosterically.

The catalytic activity of several kinases, including MAPK, PDK, and Chk2, is known to be regulated though allosteric mechanisms via binding or docking to regions on the substrate that are distinct to the phospho-acceptor site (*8*). In the case of MAP kinases, docking sites are also present on regulatory binding partners or scaffold proteins and act to tether the substrate and the kinase together. Subtle differences in the affinity of the MAPK members for these docking sites can, therefore, confer a degree of substrate selectivity and specificity. Furthermore, binding to such docking motifs can significantly enhance substrate recognition and utilization through dynamic structural or conformational alterations in and around the enzyme's active site. Enzyme interaction with docking sites can, therefore, significantly influence activity and substrate specificity and add a higher level of complexity to enzyme regulation. Allosteric interactions can also activate kinases toward substrates that do not contain canonical consensus phosphorylation sequences. Indeed, the allosteric activation of the enzyme toward weak substrates has been observed for kinases such as Chk2 (*9*). p53 does not contain a consensus Chk2 phosphorylation site; however, Chk2 activity toward the Box I transactivation domain of p53 and phosphorylation at $Thr^{18}$ and $Ser^{20}$ were enhanced by the addition of synthetic peptides corresponding to regions of the DNA binding domain of p53, Box II and Box V (*9*). Studies using ELISA revealed that Box II and Box V both bind with high affinity toward Chk2. The ability of both peptides to reconstitute Chk2 activity toward $p53^{1-66}$ *in trans* suggests Chk2 binding to sites on the substrate distinct to the actual phosphorylation site can permit utilization of substrates that possess little homology at the consensus phospho-acceptor site. Enzyme binding to a secondary site on the substrate may not be important when the substrates consensus phosphorylation site fulfils the correct criteria for efficient utilization yet would be necessary to enhance catalytic activity toward substrates that have weak conservation of residues in and around the phospho-acceptor residue.

Three regions derived from the p21 protein were able to allosterically activate both DAPK core and ZIPK activity toward the p53 mini protein, $p53^{1-66}$. An examination of the amino acid sequences of the stimulatory peptides does not reveal any striking similarity between the peptides or obvious consensus or repeat of sequence. Although the sequences covered by the peptides are not contiguous on p21, it is possible that these regions create some form of docking interface, which binds and enhances basal catalytic activity

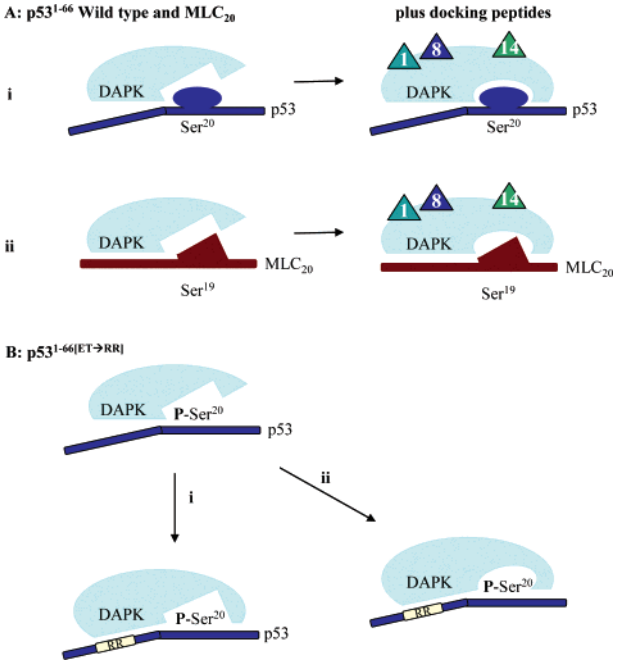


FIGURE 9: Model accounting for the modulation of DAPK activity by p21 docking peptides and basic mutations within $p53^{1-66}$. (A i) p21 docking peptides enhance DAPK binding and phosphorylation of p53 at the $Ser^{20}$ phospho-acceptor site. Interaction with the p21 docking peptides, 1, 8, and 14, creates conformational changes within the $Ser^{20}$ binding site, which clamp DAPK around p53 at $Ser^{20}$, enhancing basal $Ser^{20}$ phosphorylation. In contrast, interaction with p21 docking peptides reduces basal phosphorylation $MLC_{20}$ at Ser19 (A ii). This is possibly due to conformational changes within the active site weakening the key interactions required for $MLC_{20}$ binding and orientation and thus reducing $MLC_{20}$ phosphorylation and utilization. (B) Arginine mutations with $p53^{1-66}$ enhance DAPK core substrate utilization and catalytic efficiency. Two models may account for this: (i) Arginine mutations within $p53^{1-66}$ may enhance $p53^{1-66}$ interaction with DAPK at the substrate binding site, promoting p53 alignment and phosphorylation at $Ser^{20}$. (ii) Alternately, interaction with $p53^{1-66}$ may induce a conformational change within the active site/substrate binding pocket, improving substrate association and utilization. The latter model is favored because of data demonstrating that the apparent $K_m$ for p53 and ATP is paradoxically elevated using $p53^{1-66[ET\rightarrow RR]}$ as a substrate. Future approaches to define whether actual conformational changes occur in DAPK will include biophysical analyses to distinguish between the two models.

(Figure 9A i). Because the p21 peptides also protect DAPK and ZIPK from tryptic digestion, our findings suggest the observed increase in catalytic activity may result from conformational changes within DAPK and ZIPK generated via binding to the docking peptide interface. These changes may arise at the substrate binding site, act to enhance phosphorylation at the $Ser^{20}$ site through improved substrate interactions, and may effectively clamp p53 within the substrate binding site (Figure 9A i).

Although the p21 docking peptides were able to enhance DAPK phosphorylation of $p53^{1-66[ET\rightarrow RR]}$, the stimulatory effects of peptides 1 and 8 were not as striking as in the presence of wild-type $p53^{1-66}$. This suggests the conformational changes induced by association with peptides 1 and 8 may also promote a more complimentary alignment of p53 within the active site such that in the presence of $p53^{1-66[ET\rightarrow RR]}$, where interactions may be improved (see below), additional conformational changes within the substrate binding site are not as necessary to generate efficient $Ser^{20}$ phosphorylation. In contrast, the docking effects of peptide 14 were not affected by the mutation of $p53^{1-66}$, and peptide 14 was still able to enhance DAPK phosphorylation of $p53^{1-66[ET\rightarrow RR]}$, suggesting that peptide 14 mediates its effects on DAPK activity in a manor that is independent of any conformational changes around the $p53^{1-66}$ binding site. It is possible that peptide 14-mediated docking effects may involve subtle changes within the ATP binding pocket, influencing enzyme activity through ATP binding and utilization.

Surprisingly, although the same p21 docking peptides stimulated $p53^{1-66}$ phosphorylation, they inhibited DAPK core and ZIPK activity toward its classical substrate $MLC_{20}$. Because the docking peptides were not themselves used as substrates, these effects cannot be due to direct competition with $MLC_{20}$ at the active site. Not all docking interactions activate enzyme activity, and interaction with docking motifs can just as readily inhibit activity. Indeed, high-affinity docking sites from the tetramerization domain of p53 can bind and inhibit catalytic activity of cyclin-dependent kinase 2 (*30*). It is, however, surprising that in this study, the same set of peptides confer both activation and inhibition of DAPK and ZIPK activity. Is it, therefore, possible that docking may switch the substrate utilization of DAPK and ZIPK? A similar docking-dependent switch of Chk2 toward p53 phosphorylation without altering CDC25 phosphorylation provides another example of where enzyme specificity can be altered by a distal protein−protein interaction (*9*). By altering the conformation of the active site, substrate binding interactions maybe enhanced, leading to increased substrate utilization; however, these changes may also reduce or weaken the key interactions required for other substrates, thus decreasing utilization and inhibiting activity toward these substrates (Figure 9A ii). This switch in affinity from one consensus to another may, therefore, account for the contrasting findings for DAPK and ZIPK with p53 and $MLC_{20}$ in the presence of the peptides. Structural and biophysical studies in the presence of the docking peptides and various substrates will, however, be required to confirm this hypothesis.

Several studies have suggested that the cyclin-dependent kinase inhibitors, p21, p27, and p57, can influence actin filament organization and cytoskeletal dynamics through regulation of the Rho signaling pathway (*31*). The Rho signaling cascade critically regulates the actin cytoskeleton and cell migration, and Rho kinase controls the formation of stress fibers and focal adhesions (*32*). Rho kinase also regulates actin−myosin contractility and thereby controls smooth muscle contraction. p21, p27, and p57 act upon distinct points in the Rho signaling cascade to inhibit cell motility. Inhibition of the Rho pathway is independent of their ability to inhibit the cyclin/CDK complexes and depends on their cytoplasmic localization (*33*, *34*). Transient inhibition of the Rho cascade by CDK inhibitors is thought to permit proper cell spreading and migration. Rho kinase is a serine/threonine kinase, and its functions are achieved by phosphorylation and inhibition of the myosin binding subunit of the $MLC_{20}$ phosphatase, MYPT1, as well as direct phosphorylation of $MLC_{20}$ at $Ser^{19}$ (*31*). Studies in NIH-3T3 cells and hippocampal neurons found cytoplasmic p21 directly binds to and inhibits Rho kinase *in vitro* and *in vivo* (*33*). Inhibition of Rho kinase by p21 was concentration dependent

and correlated with the loss of stress fiber formation and increased neurite extension and branching in hippocampal neurons. DAPK and ZIPK can also target $MLC_{20}$ at $Ser^{19}$ *in vivo* (*10*, *23*, *35*) and are involved in the formation and maintenance of stress fibers (*23*, *35*). The activities of DAPK and ZIPK can, therefore, influence cell morphology and cell motility (*36*, *37*), and in addition to targeting $MLC_{20}$, DAPK achieves this through inside out modulation of integrin signaling and the formation of focal adhesions (*36*, *38*). The similarities between DAPK, ZIPK, and Rho kinase cellular function and their ability to target $MLC_{20}$ suggests that the observed inhibition of $MLC_{20}$ utilization in the presence of p21 docking peptides *in vitro* may reflect a potential role for p21 regulation of DAPK and ZIPK activity toward $MLC_{20}$ and cytoskeletal organization *in vivo*. Indeed, previous studies have suggested that phosphorylation of p21 at $Thr^{145}$ can relocate p21 to the cytoplasm (*39*). It is, therefore, possible that phosphorylation of p21 by DAPK and ZIPK at $Thr^{145}$ may account for some of the changes in cell morphology and motility generated by DAPK and ZIPK through cytoplasmic accumulation of p21 and inhibition of Rho and DAPK signaling to the cytoskeleton. Analyses of the effect of peptides on cytoskeletal organization and cell motility *in vivo* will be required to clarify this.

In this study, we found that ZIPK was dramatically less active than DAPK core toward substrates such as p53 and $MLC_{20}$, even though the phosphorylation of p21 and $MLC_{20}$ peptide substrate was comparable to that of DAPK core. The weak activity of ZIPK toward $MLC_{20}$ was surprising because ZIPK is known to di-phosphorylate $MLC_{20}$ *in vitro* and *in vivo* at $Thr^{18}$ and $Ser^{19}$ and is responsible for agonist-induced smooth muscle contraction (*24*). Indeed, ZIPK can phosphorylate $MLC_{20}$ more efficiently than myosin light chain kinase (*40*). The low levels of ZIPK activity observed here may, however, be due to the use of full-length ZIPK purified from bacteria. Unlike DAPK-1, ZIPK lacks a calmodulin regulatory domain and is not subject to regulation by CaM. Instead, ZIPK appears to be positively regulated by phosphorylation, and this can influence both ZIPK activity and subcellular localization (*41*). It is, therefore, possible that the observed low levels of ZIPK activity may be due to a lack of post-translational modification and phosphorylation at key residues such as $Thr^{180}$, $Thr^{225}$, and $Thr^{265}$. The COOH-terminal domain of ZIPK also appears to contain a regulatory or inhibitory domain because the removal of the C-terminus by truncation of ZIPK at residues 273 or 342 dramatically increased ZIPK activity (*41*). Because the DAPK core construct used in this study contains residues 1−278 and DAPK and ZIPK share high degree of homology within this region, these findings suggest that the regulatory function of the COOH domain may involve substrate interaction or recognition. Although full-length ZIPK may have higher order structural complications, the specific activity of DAPK core and ZIPK were similar toward p21 protein (Figure 1B and G), p21 peptide 13 (Figure 1D), MLC peptide substrate (Figure 2B), and p53-stimulation (Figure 3A and B). As such, this data suggests that the DAPK core and full-length ZIPK share characteristics with respect to the p21-peptide docking reaction.

The p53 tumor suppressor protein is subject to complex and diverse combinations of post-translational modification, which can markedly influence its activity as a transcription factor by modifying its activity, stability, and interaction with binding partners. Seventeen serine and threonine phosphorylation sites on p53 have been detected in human cells, and many of these are clustered in the trans-activation domain. These sites are targeted in response to diverse forms of DNA damage and stress by various kinases, including casein kinase (CK) 1 and 2, ATM, ATR, DNA-PK, Chk1, and Chk2 (*42*). Although certain sites are known to be targeted by a single kinase, significant overlap occurs, and certain sites are known to be targeted by many kinases. Specificity is thus required and is achieved through enzyme affinity for the amino acid sequence surrounding the phospho-acceptor residue as well as interplay between the phosphorylation sites. For example, CK1 phosphorylates p53 at $Thr^{18}$; however, this requires prior phosphorylation at $Ser^{15}$ by DNA-PK (*43*) to create the correct docking site for CK1 and prime CK1 to target and phosphorylate $Thr^{18}$.

Although only one or two residues are modified by enzymes at the active site, the residues surrounding the phospho-acceptor residue can significantly contribute to substrate binding through hydrophobic and noncovalent interactions. Characterization of the catalytic properties of DAPK toward synthetic peptide substrates and phage display panning for binding peptides have given insights into the consensus binding sequence of the DAPK family members (*11*, *22*). These studies have shown that DAPK/ZIPK has a preference for basic residues such as arginine and lysine upstream of the serine/threonine phosphorylation site (*11*). Downstream of the phospho-acceptor site, substrates targeted by DAPK members appear to be rich in hydrophobic residues, such as leucine, valine, and phenylalanine (Figure 1). Mutation of these residues to alanine stimulated ZIPK activity toward peptide p21 3-fold (*22*). These data suggest that DAPK family members have a large contact site with substrates, and modulation of the residues within this site may influence binding affinity and the efficiency of substrate utilization.

The importance of the basic residues upstream of the phospho-acceptor residue has been highlighted by mutational analyses. Mutation of lysine to alanine in the basic cluster greatly reduced peptide−substrate utilization by DAPK *in vitro* by approximately half (*11*). Here, we show that the mutant form of $p53^{1-66}$ containing arginine insertions at codons 17 and 18 was far more efficiently used as a substrate by DAPK core and ZIPK than wild-type $p53^{1-66}$. This was seen as a ∼40-fold increase in $V_{max}$ compared to that of the wild type and a ∼2-fold increase in DAPK core catalytic efficiency. Changes in the consensus site of $p53^{1-66}$ appear to be specific for DAPK and ZIPK because phosphorylation of $p53^{1-66[ET\rightarrow RR]}$ by Chk2 was not dramatically greater than that of wild-type $p53^{1-66}$. Indeed a comparison of the sequences of several Chk2 substrates suggests that Chk2 has a distinct consensus phosphorylation sequence (L-X-R-X-X-S/T), which does not appear to require a high proportion of basic residues (*44*).

Two mechanisms may account for the increase in DAPK core catalytic efficiency in the presence of $p53^{1-66[ET\rightarrow RR]}$ (Figure 9B). First, the arginine mutations within $p53^{1-66}$ may enhance $p53^{1-66[ET\rightarrow RR]}$ interaction with DAPK and binding at the substrate active site, promoting $p53^{1-66[ET\rightarrow RR]}$ alignment and phosphorylation at $Ser^{20}$ (Figure 9B i). The crystal structure of the DAPK catalytic domain has been solved by

mapping onto phosphorylase kinase and the use of a docked peptide substrate model uncovered the potential amino acids involved in substrate recognition (*11*, *12*). Two clusters of acidic glutamic acid residues were identified at the predicted substrate binding site, and it is suggested that these residues may interact with and compliment the basic charge of residues upstream of the phospho-acceptor site (*11*). It is, therefore, possible that the increased basic residue content of $p53^{1-66[ET\rightarrow RR]}$ creates stronger interactions with the key glutamic acid residues within the substrate binding pocket, promoting more optimal alignment of $p53^{1-66[ET\rightarrow RR]}$ at the active site such that the phosphorylation of $Ser^{20}$ is increased. However, the $V_{max}$ and $k_{cat}/K_m$ values for ATP in the presence of $p53^{1-66[ET\rightarrow RR]}$ were also greater than those of DAPK core in the presence of wild-type $p53^{1-66}$, suggesting that $p53^{1-66[ET\rightarrow RR]}$ also improves DAPK consumption of ATP. This suggests that$p53^{1-66[ET\rightarrow RR]}$ may increase DAPK core activity by influencing the conformation of the active site/substrate binding pocket (Figure 9B ii), thus improving specific activity through enhanced association and utilization of both $p53^{1-66}$ and ATP via some form of induced fit. Surprisingly, the increase in $V_{max}$ for $p53^{1-66[ET\rightarrow RR]}$ and ATP was accompanied by a large increase in the $K_m$ value for both substrates. It is unknown why this is the case; however, this may reflect an increase in the strength of enzyme−substrate interaction, reducing or preventing the dissociation of the product from the active site. In spite of this, the catalytic efficiency of the DAPK core in the presence of $p53^{1-66[ET\rightarrow RR]}$ is still far greater than that of the wild-type $p53^{1-66}$, confirming that altering the basic residue content of the 5′ region of p53 $Ser^{20}$ consensus site greatly improves $p53^{1-66}$ utilization by DAPK core and ZIPK. This was recapitulated in cell systems, where the ET−RR full-length p53 mutant was a better substrate *in vivo* for a Ser20 kinase.

The specific positioning of the basic residues within the consensus sequence may also influence substrate utilization by DAP and ZIP kinase. $MLC_{20}$ and p21 are both rich in lysine and arginine residues down stream of the phosphorylated residue (Figure 1); however, phosphorylation of p21 by both DAPK and ZIPK was far greater than that of $MLC_{20}$. This suggests that there may be specific conformational constraints within the DAPK and ZIPK binding sites and optimal points of interaction with the substrate in the binding pocket. The proline and glutamine residues located between the basic residues and the phospho-acceptor serine of $MLC_{20}$ may, therefore, weaken these interactions, reducing binding at the active site and, therefore, phosphorylation of $MLC_{20}$. The conformational changes imposed by the docking peptides may further weaken any tenuous interactions such that inhibition of DAPK and ZIPK targeting of $MLC_{20}$ occurs.

The COOH-terminal region of p21 interacts with several proteins and ligands, including PCNA, CDK, CaM, the oncoprotein, SET, and the C8 subunit of the proteasome (*45*). It is, therefore, possible that the p21 docking peptides such as peptide 14 may interact with the endogenous binding partners of p21 and perturb their function, making it difficult to dissect the effects caused by docking peptide modulation of DAPK activity. NMR and CD analysis has shown that p21 is a highly disordered polypeptide with very little secondary or tertiary structure (*46*). However, p21 appears to be very dynamic and can adopt an ordered conformation upon binding to its interaction partners such as CDK. Moreover, structural studies reveal that peptides corresponding to the COOH-terminus of p21 region are capable of adopting multiple structural conformations depending on their environment and binding partner and also showed that it was possible to prime peptides to adopt a particular conformation and thus specificity of interaction through mutation of the amino acid backbone (*47*). It may, therefore, be possible to make structural alterations within the docking peptides so that only conformations specific for DAPK and ZIPK interaction and stimulation are achieved *in vivo*. Truncated versions of the docking peptides showed slight differences in the precise docking interface created between peptide 8 and DAPK and ZIPK. It may, therefore, be feasible to generate docking peptides specific to DAPK or ZIPK such that targeted delineation of these pathways can be achieved, and thus, the relative importance of DAPK or ZIPK in cell processes such as morphological changes during normal growth and apoptotic cell death can be determined.

In conclusion, we have reported on a chemical genetics approach to develop small peptide-mimetic ligands to manipulate how a kinase functions. This approach is based on the growing realization that the information built into a protein kinase to target a phospho-acceptor site is not confined to active site−substrate interactions. Rather, docking interfaces out with the active site can alter the conformation, affinity, or specificity of a kinase domain toward a substrate. DAPK-1 was used as a model enzyme to develop selective ligands that modulate its specific activity, and our data suggest that DAPK-1 binding ligands can be generated and can be used in the future to drive assay development designed to alter DAPK-1-specific activity *in vivo*.

## REFERENCES

1. Walsh, D. P., and Chang, Y. T. (2006) Chemical genetics, *Chem. Rev. 106*, 2476−2530.
2. Gibbs, J. B., Oliff, A., and Kohl, N. E. (1994) Farnesyltransferase inhibitors: Ras research yields a potential cancer therapeutic, *Cell 77*, 175−178.
3. Ball, K. L., Lain, S., Fahraeus, R., Smythe, C., and Lane, D. P. (1997) Cell-cycle arrest and inhibition of Cdk4 activity by small peptides based on the carboxy-terminal domain of p21WAF1, *Curr. Biol. 7*, 71−80.
4. Fahraeus, R., Paramio, J. M., Ball, K. L., Lain, S., and Lane, D. P. (1996) Inhibition of pRb phosphorylation and cell-cycle progression by a 20-residue peptide derived from p16CDKN2/INK4A, *Curr. Biol. 6*, 84−91.
5. Bottger, A., Bottger, V., Sparks, A., Liu, W. L., Howard, S. F., and Lane, D. P. (1997) Design of a synthetic Mdm2-binding mini protein that activates the p53 response in vivo, *Curr. Biol. 7*, 860−869.
6. Friedler, A., Hansson, L. O., Veprintsev, D. B., Freund, S. M., Rippin, T. M., Nikolova, P. V., Proctor, M. R., Rudiger, S., and Fersht, A. R. (2002) A peptide that binds and stabilizes p53 core domain: chaperone strategy for rescue of oncogenic mutants, *Proc. Natl. Acad. Sci. U.S.A. 99*, 937−942.
7. Wallace, M., Worrall, E., Pettersson, S., Hupp, T. R., and Ball, K. L. (2006) Dual-site regulation of MDM2 E3-ubiquitin ligase activity, *Mol. Cell 23*, 251−263.
8. Biondi, R. M., and Nebreda, A. R. (2003) Signalling specificity of Ser/Thr protein kinases through docking-site-mediated interactions, *Biochem. J. 372*, 1−13.
9. Craig, A., Scott, M., Burch, L., Smith, G., Ball, K., and Hupp, T. (2003) Allosteric effects mediate CHK2 phosphorylation of the p53 transactivation domain, *EMBO Rep. 4*, 787−792.
10. Bialik, S., Bresnick, A. R., and Kimchi, A. (2004) DAP-kinase-mediated morphological changes are localization dependent and involve myosin-II phosphorylation, *Cell Death Differ. 11*, 631−644.

11. Velentza, A. V., Schumacher, A. M., Weiss, C., Egli, M., and Watterson, D. M. (2001) A protein kinase associated with apoptosis and tumor suppression: structure, activity, and discovery of peptide substrates, *J. Biol. Chem. 276*, 38956−38965.
12. Tereshko, V., Teplova, M., Brunzelle, J., Watterson, D. M., and Egli, M. (2001) Crystal structures of the catalytic domain of human protein kinase associated with apoptosis and tumor suppression, *Nat. Struct. Biol. 8*, 899−907.
13. Velentza, A. V., Schumacher, A. M., and Watterson, D. M. (2002) Structure, activity, regulation, and inhibitor discovery for a protein kinase associated with apoptosis and neuronal death, *Pharmacol. Ther. 93*, 217−224.
14. Yamamoto, M., Hioki, T., Ishii, T., Nakajima-Iijima, S., and Uchino, S. (2002) DAP kinase activity is critical for C(2)-ceramide-induced apoptosis in PC12 cells, *Eur. J. Biochem. 269*, 139−147.
15. Shamloo, M., Soriano, L., Wieloch, T., Nikolich, K., Urfer, R., and Oksenberg, D. (2005) Death-associated protein kinase is activated by dephosphorylation in response to cerebral ischemia, *J. Biol. Chem. 280*, 42290−42299.
16. Schumacher, A. M., Velentza, A. V., and Watterson, D. M. (2002) Death-associated protein kinase as a potential therapeutic target, *Expert Opin. Ther. Targets 6*, 497−506.
17. Schori, H., Yoles, E., Wheeler, L. A., Raveh, T., Kimchi, A., and Schwartz, M. (2002) Immune-related mechanisms participating in resistance and susceptibility to glutamate toxicity, *Eur. J. Neurosci. 16*, 557−564.
18. Pelled, D., Raveh, T., Riebeling, C., Fridkin, M., Berissi, H., Futerman, A. H., and Kimchi, A. (2002) Death-associated protein (DAP) kinase plays a central role in ceramide-induced apoptosis in cultured hippocampal neurons, *J. Biol. Chem. 277*, 1957−1961.
19. Velentza, A. V., Wainwright, M. S., Zasadzki, M., Mirzoeva, S., Schumacher, A. M., Haiech, J., Focia, P. J., Egli, M., and Watterson, D. M. (2003) An aminopyridazine-based inhibitor of a pro-apoptotic protein kinase attenuates hypoxia-ischemia induced acute brain injury, *Bioorg. Med. Chem. Lett. 13*, 3465−3470.
20. Bradford, M. M. (1976) A rapid and sensitive method for the quantitation of microgram quantities of protein utilizing the principle of protein-dye binding, *Anal. Biochem. 72*, 248−254.
21. Scott, M. T., Ingram, A., and Ball, K. L. (2002) PDK1-dependent activation of atypical PKC leads to degradation of the p21 tumour modifier protein, *EMBO J. 21*, 6771−6780.
22. Burch, L. R., Scott, M., Pohler, E., Meek, D., and Hupp, T. (2004) Phage-peptide display identifies the interferon-responsive, death-activated protein kinase family as a novel modifier of MDM2 and p21WAF1, *J. Mol. Biol. 337*, 115−128.
23. Kuo, J. C., Lin, J. R., Staddon, J. M., Hosoya, H., and Chen, R. H. (2003) Uncoordinated regulation of stress fibers and focal adhesions by DAP kinase, *J. Cell Sci. 116*, 4777−4790.
24. Niiro, N., and Ikebe, M. (2001) Zipper-interacting protein kinase induces Ca(2+)-free smooth muscle contraction via myosin light chain phosphorylation, *J. Biol. Chem. 276*, 29567−29574.
25. Unger, T., Juven-Gershon, T., Moallem, E., Berger, M., Vogt Sionov, R., Lozano, G., Oren, M., and Haupt, Y. (1999) Critical role for Ser20 of human p53 in the negative regulation of p53 by Mdm2, *EMBO J. 18*, 1805−1814.
26. Dornan, D., and Hupp, T. R. (2001) Inhibition of p53-dependent transcription by BOX-I phospho-peptide mimetics that bind to p300, *EMBO Rep. 2*, 139−144.
27. Cohen, O., Feinstein, E., and Kimchi, A. (1997) DAP-kinase is a Ca2+/calmodulin-dependent, cytoskeletal-associated protein kinase, with cell death-inducing functions that depend on its catalytic activity, *EMBO J. 16*, 998−1008.
28. Shohat, G., Spivak-Kroizman, T., Cohen, O., Bialik, S., Shani, G., Berrisi, H., Eisenstein, M., and Kimchi, A. (2001) The pro-apoptotic function of death-associated protein kinase is controlled by a unique inhibitory autophosphorylation-based mechanism, *J. Biol. Chem. 276*, 47460−47467.
29. Llambi, F., Lourenco, F. C., Gozuacik, D., Guix, C., Pays, L., Del Rio, G., Kimchi, A., and Mehlen, P. (2005) The dependence receptor UNC5H2 mediates apoptosis through DAP-kinase, *EMBO J. 24*, 1192−1201.
30. Luciani, M. G., Hutchins, J. R., Zheleva, D., and Hupp, T. R. (2000) The C-terminal regulatory domain of p53 contains a functional docking site for cyclin A, *J. Mol. Biol. 300*, 503−518.
31. Fukata, Y., Amano, M., and Kaibuchi, K. (2001) Rho-Rho-kinase pathway in smooth muscle contraction and cytoskeletal reorganization of non-muscle cells, *Trends Pharmacol. Sci. 22*, 32−39.
32. Amano, M., Chihara, K., Kimura, K., Fukata, Y., Nakamura, N., Matsuura, Y., and Kaibuchi, K. (1997) Formation of actin stress fibers and focal adhesions enhanced by Rho-kinase, *Science 275*, 1308−1311.
33. Tanaka, H., Yamashita, T., Asada, M., Mizutani, S., Yoshikawa, H., and Tohyama, M. (2002) Cytoplasmic p21(Cip1/WAF1) regulates neurite remodeling by inhibiting Rho-kinase activity, *J. Cell Biol. 158*, 321−329.
34. Besson, A., Gurian-West, M., Schmidt, A., Hall, A., and Roberts, J. M. (2004) p27Kip1 modulates cell migration through the regulation of RhoA activation, *Genes Dev. 18*, 862−876.
35. Murata-Hori, M., Suizu, F., Iwasaki, T., Kikuchi, A., and Hosoya, H. (1999) ZIP kinase identified as a novel myosin regulatory light chain kinase in HeLa cells, *FEBS Lett. 451*, 81−84.
36. Kuo, J. C., Wang, W. J., Yao, C. C., Wu, P. R., and Chen, R. H. (2006) The tumor suppressor DAPK inhibits cell motility by blocking the integrin-mediated polarity pathway, *J. Cell Biol. 172*, 619−31.
37. Komatsu, S., and Ikebe, M. (2004) ZIP kinase is responsible for the phosphorylation of myosin II and necessary for cell motility in mammalian fibroblasts, *J. Cell Biol. 165*, 243−254.
38. Wang, W. J., Kuo, J. C., Yao, C. C., and Chen, R. H. (2002) DAP-kinase induces apoptosis by suppressing integrin activity and disrupting matrix survival signals, *J. Cell Biol. 159*, 169−179.
39. Rossig, L., Jadidi, A. S., Urbich, C., Badorff, C., Zeiher, A. M., and Dimmeler, S. (2001) Akt-dependent phosphorylation of p21-(Cip1) regulates PCNA binding and proliferation of endothelial cells, *Mol. Cell. Biol. 21*, 5644−5657.
40. Murata-Hori, M., Fukuta, Y., Ueda, K., Iwasaki, T., and Hosoya, H. (2001) HeLa ZIP kinase induces diphosphorylation of myosin II regulatory light chain and reorganization of actin filaments in nonmuscle cells, *Oncogene 20*, 8175−8183.
41. Graves, P. R., Winkfield, K. M., and Haystead, T. A. (2005) Regulation of zipper-interacting protein kinase activity in vitro and in vivo by multisite phosphorylation, *J. Biol. Chem. 280*, 9363−9374.
42. Bode, A. M., and Dong, Z. (2004) Post-translational modification of p53 in tumorigenesis, *Nat. Rev. Cancer 4*, 793−805.
43. Dumaz, N., Milne, D. M., and Meek, D. W. (1999) Protein kinase CK1 is a p53-threonine 18 kinase which requires prior phosphorylation of serine 15, *FEBS Lett. 463*, 312−316.
44. Stevens, C., Smith, L., and La Thangue, N. B. (2003) Chk2 activates E2F-1 in response to DNA damage, *Nat. Cell Biol. 5*, 401−409.
45. Dotto, G. P. (2000) p21(WAF1/Cip1): more than a break to the cell cycle? *Biochim. Biophys. Acta 1471*, M43−M56.
46. Kriwacki, R. W., Hengst, L., Tennant, L., Reed, S. I., and Wright, P. E. (1996) Structural studies of p21Waf1/Cip1/Sdi1 in the free and Cdk2-bound state: conformational disorder mediates binding diversity, *Proc. Natl. Acad. Sci. U.S.A. 93*, 11504−11509.
47. Esteve, V., Canela, N., Rodriguez-Vilarrupla, A., Aligue, R., Agell, N., Mingarro, I., Bachs, O., and Perez-Paya, E. (2003) The structural plasticity of the C terminus of p21Cip1 is a determinant for target protein recognition, *ChemBioChem 4*, 863−869.


BI061562J